Stony Brook University

Hudson River Estuary sedimentary evolution: A multiyear comparison and analysis of multibeam sonar surveys

A Thesis Presented

by

Tobias John Vincent Hatten

To

The Graduate School

In Partial Fulfillment of the

Requirements

For the Degree of

Master of Science

in

Marine and Atmospheric Science

(Marine Geology)

Stony Brook University

May 2010

Stony Brook University

The Graduate School

Tobias John Vincent Hatten

We, the thesis committee for the above candidate for the

Master of Science degree, hereby recommend

acceptance of this thesis.

Roger Flood - Thesis Advisor
Professor of Marine and Atmospheric Science

Henry Bokuniewicz - Thesis committee member
Professor of Marine and Atmospheric Science

Robert Wilson - Thesis committee member
Associate Professor of Marine and Atmospheric Science

This thesis is accepted by the Graduate School

Lawrence Martin
Dean of the Graduate School

Abstract of the thesis

Hudson River Estuary sedimentary evolution: A multiyear comparison and analysis of multibeam sonar surveys

by

Tobias John Vincent Hatten

Master of Science

In

Marine and Atmospheric Science
(Marine Geology)

Stony Brook University
2010

Hudson River multibeam sonar surveys were conduced between New York City, NY and Hudson, NY in 1998 to 2003 and in 2005 as part of the Hudson River Benthic Mapping Project 1998 to 2003 and NOAA's Office of Exploration 2005. Data from these surveys were compared and used to identify areas where morphological river bed change occurred. The comparison of surveys identified sand wave migration rates ranging from 1-7 m/year in both the northern and southern sections of the river and produced examples of human induced change such as anchor drags and dredge spoils. These findings suggest that there have been changes in water depth, and that more frequently surveys should be done to identify patterns of change, highest resolution techniques should be employed to limit future errors, and additional tidal measurements would help increase vertical accuracy in the 2005 data set. In particular, techniques such as RTK GPS navigation systems would also increase survey accuracy.

Table of Contents

List of Tables ……..……..……v
List of Figures……..vi
Acknowledgements……vii
1. Introduction……1
2. Research Objectives……4
3. Hudson River Estuary Setting/Physical Description……6
    a. Tidal and River Influence……..……6
    b. Hudson River Geologic Setting……7
    c. Hudson River Estuary Classification ……..……9
4. Cultural Significance of the Hudson River……11
5. Previous Research……12
    a. Acoustic Sounding Techniques……12
    b. Hudson River Research……13
    c. Sand Wave Migration……..……14
    d. Short Term Geomorphic Change Studies……17
6. Research Methods……19
    a. Bathymetric Data Reductions……21
    b. System Limitations……24
        i. Horizontal Limitations……..……...24
        ii. Vertical Limitations……..……25
    c. Analysis……26
7. Results……28
    a. Sand Waves……28
    b. Depressions……..33
    c. Anthropogenic Features……35
        i. Protrusions……..……35
        ii. New Mounds……37
        iii. Anchor Drags……..……...39
    d. Systematic/Survey Errors /Observations..……39
8. Discussion of Results……41
    a. Sand Waves……41
    b. Anthropogenic Effects……45
9. Future Work……..……48
10. Conclusion……49
References……50
Appendix 1……57
Appendix 2……66

List of Tables

1. Map Zone Box Coordinates.....58
2. Tide Zone Box Coordinates.....60
3. Locations of USGS Tide Gauges and Tide Zone Specifications.....62
4. USGS Tide Data and NOAA Model Calculation Examples.....64

List of Figures

1. Map of Study Area (including survey regions).....67
2. Photographs of Research Vessels: Seawolf, Prichard, and Onrust.....69
3. Map of Tidal Zones.....71
4. USGS Tide Data vs. NOAA tide model plot.....73
5. PN8 Sand Wave Migration a.....75
6. PN8 Sand Wave Migration b.....77
7. PN7 Sand Wave Migration 79
8. PN7 3-d Sand Wave Migration.....81
9. PN6 Sand Wave Migration.....83
10. PN4 Isolated Sand Ridge Migration.....85
11. WS6 Sand Wave Stagnant a.....87
12. WS6 Sand Wave Stagnant b.....87
13. WS7 Sand Wave Stagnant.....89
14. PN8 Erosion Hole.....91
15. PN6 Depression Fills in.....93
16. PN4 Steep Slope Fills in.....95
17. PN7 Shipwreck Accretion Upstream.....97
18. PN6 Shipwreck Accretion South East.....99
19. PN3 Shipwreck Accretion Upstream.....101
20. PN1 Bridge and Pipe Effects.....103
21. WO Large Mound Appears.....105
22. WS7 Mound Formation.....107
23. PN2 Bulbous New Feature.....109
24. PS1 Anchor Drag Evidence.....111
25. PO Example of Systematic Offset.....113
26. van Rijn Graph of water depth vs. critical velocity 115

Acknowledgements

I would first like to thank my advisor Dr. Roger Flood for his never-ending support towards the completion of my thesis project. Dr. Flood always offered constructive criticism and much needed encouragement. I would also like to thank Dr. Flood for introducing me to the Hudson River project and obtaining necessary funding and permissions. Dr. Flood showed me how persistence equates to achievement. These skills will prove valuable for years to come.

I would like to thank my thesis committee members Dr. Henry Bokuniewicz and Dr. Robert Wilson for their time, efforts and advice. Their keen eyes have allowed me to view the research from a new perspective and have strengthened my thesis. Their viewpoints have demonstrated the value of empathy. This need to listen and understand many points of view will be a valuable lesson that I will take with me.

During my studies I was supported by a Stony Brook University Teaching Assistantship and Graduate Assistantship. The Stony Brook University Assistantships were funded by the New York State Department of Environmental Conservation Memorandum of understanding Grant AM06778 and the National Oceanographic and Atmospheric Administration Office of Exploration: Understanding the Maritime History of the Lower Hudson River Grant NAØ70AR4600294. During the final year at Stony Brook University I was supported by The Carroll & Milton Petrie Foundation Scholarship Loan Program.

The initial (1998-2003) Hudson River research was funded by The New York State Department of Environmental Conservation Memorandum of understanding Grant AM06778. The 2005 Hudson River data were funded by The National Oceanographic and Atmospheric Administration Office of Exploration: Understanding the Maritime History of the Lower Hudson River Grant NAØ70AR4600294. These funding sources have been invaluable towards advancing the understanding of the Hudson River and preserving the immense cultural riches.

I would like to thank the Hudson River Project Researchers, faculty, students, and staff who spent thousands of hours collecting and processing the bathymetry data which my project has been based upon. Without their tireless work, my project would not have occurred.

I would also like to thank Juliet Kinney from SoMAS for her support, guidance and wisdom in the Flood lab. Her ability to listen and help solve difficult problems was invaluable. Without her help I would not have been able to complete this project. Also, thank you to the staff, faculty, teachers, and students for their support and motivation!

I would finally like to thank my family, my wife Annie and dog Wicket for their cheers, encouragement and understanding. Last but not least I would like to thank my Parents, Kenneth and Mary Louise Hatten for always asking “Is your thesis done yet?”. Their edits have finally made my project complete!

1. Introduction:

Multiple precision multi-beam sonar bathymetry surveys give new insights into benthic processes on a multiannual scale. Between 1998 and 2005 an exhaustive series of multi-beam surveys in the Hudson River were collected covering 150 km of river between New York City, and Troy, New York (Figure 1, Table 1). Acoustic surveys of the Hudson River Valley are a valuable resource documenting changing conditions (Carbotte et al. 2004).

The first multi-beam study was conducted from 1998 to 2003 by researchers from the School of Marine and Atmospheric Sciences (SoMAS) at Stony Brook University, while researchers from the Lamont Doherty Earth Research Institute at Columbia University, and Queens College collected side-scan sonar, seismic profiles, and sediment cores as part of the New York State Department of Environmental Conservation (NYSDEC) Hudson River Benthic Mapping Program (Bell et al. 2000, 2003; Carbotte et al. 2004). The goal of this program was to provide a regional framework of Hudson River benthic environments for regional planners (Carbotte et al. 2004). A second multi-beam study was conducted in 2005 by SoMAS funded by NOAA's Office of Exploration.

The Hudson River multi-beam study from 1998 to 2003 was conducted using the Research Vessels R/V Onrust, R/V Prichard and R/V Seawolf owned and operated by SoMAS (Figure 2). These vessels were equipped with a Simrad EM3000 multi-beam sonar bathymetric system. The second multi-beam study conducted in 2005 utilized the R/V Seawolf (Figure 2). This vessel was equipped with a higher resolution Reson 8125 multi-beam bathymetric system. The survey from 1998 to 2003 covered the entire river area between New York City and Troy, NY while the survey of 2005 was a single line from New York City to Hudson, NY. The data from 1998 to 2003 were gridded at 1m resolution as a GIS base map by SoMAS investigators involved in the Hudson River Benthic Mapping project. Data from 2005 were edited and corrected using the computer program CARIS HIPS and SIPS then plotted for use in ArcView GIS by Hatten at Stony Brook University.

An extensive range of research projects have been conducted in the Hudson River, including numerous projects on morphology and the river bed's sedimentary characteristics (Nitsche et al 2007, 2004). However, this is the first study to examine short term morphological changes in the Hudson River. With the new data set, an opportunity to study morphological change where the surveys overlapped was presented. Due to the high resolution of the Hudson River surveys numerous examples of morphologic change can be observed and will be reported.

In the following sections the methods used to collect and process the Hudson River multi-beam surveys will be described. The discussion will include the process of analyzing the surveys, and the methods used to compare the bathymetric data. This will conclude with a discussion of observed temporal morphological evolution of the Hudson River between New York City and Hudson, NY (Figure 1, Table 1).

2. Research Objectives:

The objective of this project is to document the temporal variability in Hudson River sediments and anthropogenic features using multi-beam bathymetric survey data. The extent of change of sedimentary bedforms and features around anthropogenic objects will be recorded to help understand natural and human induced evolution of the Hudson River.

The sedimentation rate in the Hudson River is 1-3 mm/year on average (Olsen et al. 1978) due to both marine and terrestrial sediment input. This modest rate of sedimentation presents difficulties when trying to establish what the accumulated sedimentation was between the 1998 to 2003 and 2005 surveys. Factors such as bioturbation, dating accuracy, and limited vertical resolutions of 1-10 cm (Peteet and Wong 2000; Geyer et al. 2001) all complicate the study.

Since this study compares two data sets collected from 2-7 years apart this indicates that only a 2-21 mm average depth change should occur if Olsen et al. (1978) is correct. Small changes such as this are difficult to resolve in certain locations due to the limited vertical resolutions of the survey equipment which is 10 cm. To avoid this constraint, as a consequence, this research will be focused on morphological changes in the Hudson River greater than 30 cm between the survey dates.

The surveys in this study are from 1998 to 2003 and 2005 as noted. And, although bathymetry data from the initial Hudson River Benthic Mapping Project 1998 to 2003 have been studied extensively (Nitsche et al. 2007), a study of morphological changes utilizing the new data has not been done. Thus, this study will add to the current body of research that began with the Hudson River Benthic Mapping project in 1998.

3. Hudson River Estuary Setting/ Physical Description

The Hudson River is a 507 km long river that begins in the Adirondack Mountains and travels south into New York Harbor through the Battery, New York City (Nitsche et al. 2007). The Hudson River Estuary stretches 240 km upstream of New York Harbor to Troy, NY where a dam prevents any further tidal inundation (Figure 1) (Nitsche et al. 2007). The Hudson River Estuary is a mixed, tide-dominated, mesotidal estuary (Weiss 1974; Olsen et al. 1978). The width of the Hudson River Estuary varies from less than 1 km to more than 6 km (Nitsche et al. 2007).

3.a. Tidal and River Influence

The Hudson River Estuary, that is the section of the river south of the Troy Dam, is a partially mixed, tide dominated mesotidal estuary with an average tidal current of 0.5-1 m/s (Abood, 1974; Olsen et al. 1978; Geyer et al. 2000). The average tidal flux is 12,000 m^3/second; the average freshwater input from the Troy dam is much smaller at 500-700 m^3/second (Olsen et al. 1978). Thus, the average daily tidal flux of the Hudson River Estuary is 10-100 times larger than the average daily volume of freshwater influx from Hudson River tributaries (Nitsche et al. 2006).

The volume of freshwater input, however, is quite variable. Approximately 80% of the freshwater and 98% of sediments in the Hudson River are input by the Mohawk River and Upper Hudson entering north of the Troy Dam (Cooper et al. 1988; Water Resource Data 1977). The remaining ~20% of freshwater in the Hudson River is input from smaller tributaries and rivers south of the Troy Dam (Nitsche et al. 2006). Maximum river discharge volumes normally occur in the spring due to snowmelt and in the fall due to extensive rains (Nitsche et al. 2006; Menon et al. 1998). These seasonal freshwater inputs have large influence on northern infiltration of the saltwedge which is defined as 100 mg salt/liter of water (Abood 1974). The salt wedge moves between 30-90 km upstream of the Battery between Haverstraw Bay and Newburgh Bay (Abood 1974; Geyer and Chant 2006; Nitshce et al. 2006) as the river's freshwater inflow waxes and wanes.

3.b. Hudson River Geologic Setting:

The Hudson River Estuary stretches 240 km from New York City to the Federal Dam in Troy, NY (Figure 1) (Nitsche et al. 2007). The depth of the Hudson River ranges from 20-30 m in the main channel, and 0-4 m along the banks of the river. In the deepest sections, the river depth can reach 60 m (Nitsche et al. 2004).

The Hudson River Valley was carved by glaciers during the Pleistocene (Newman et al. 1969). Its current shape may be the morphological product of the Laurentide ice sheet and its retreat to the North may have carved out its deepest valleys (up to 60 m deep). Of course it may have had a similar form prior to the most recent glaciations of the Pleistocene (Isachsen et al., 2000; Sirkin and Bokuniewicz, 2006). However, when the continental ice sheet receded, the river was dammed by heterogeneous glacial debris (Uchupi et al. 2001; Donnelly et al. 2005). Next, lake bursts circa 18,000 to 14,000 years ago drained these glacially-derived lakes (Uchupi et al. 2001; Donnelly et al. 2005). Subsequently, the rising sea level flooded the valley to produce the present Hudson River (Weiss 1974).

After adjustments for post glacial rebound, sea level has been rising 1.5 mm/year in the Hudson River (Peltier 1998; Carbotte et al. 2004). This estimate is derived from geological paleo-water level data in the Hudson River (Peltier 1998). Recent salt marsh accretion rate studies of the Hudson River at Piermont, NY confirm with these estimates and suggest an accretion rate of 2-3 mm per year (Peteet and Wong 2000). These data also suggest that sea level rise in the Hudson River has been gradual during the Holocene epoch (Carbotte et al. 2004).

3.c. Hudson River Estuary Classification

Estuaries are classified in accord with their morphologies, tidal influence, wave influence, and river flow since these factors influence estuary sedimentation (Nichols and Biggs 1985; Darymple et al. 1992; Bird 2000). Typically, coastal plain estuaries, which dominate the land forms south of the Hudson River, are described as having sandy sediments at the mouth of the river, mud dominated sediments in the middle section of the river and fluvial sands and coarser material in the upper river (Nitsche et al. 2006; Dalrymple et al. 1992). Estuaries north of the Hudson River are often rock framed and of glacial origin (Nitsche et al. 2006).

The Hudson River is best classified as a coastal plain estuary in terms of sediment classification; since its mouth consists primarily of wave and tidally derived sands, the center section consists of muds, and the upper section consists primarily of fluvial derived sands (Nitsche et al. 2006). This general classification usually suits coastal plain settings, but since the Hudson River is also a heavily settled rock framed estuary, local sedimentation patterns can vary largely depending on such factors as on riverbed shape, bedrock, tributaries, and human influence (Nichols and Biggs 1985). In select locations

the Hudson River sedimentation patterns are similar to a glacially formed estuary or fjord because its bedrock framed shape (Nitsche et al. 2006).

In the Hudson River, the sediment ranges in size from 2 mm granule (-2 φ) to 3.9 μm, clay (8 φ) (Nitsche et al. 2007). In the regions where sediment waves are observed, near Yonkers and in the northern sections of the study area, sand is the majority sediment type (Nitsche et al. 2007). The sediment wave dominant areas range in grain size from 2 mm, very course sand (-1 φ) to 125 μm, very fine sand (4 φ) (Nitsche et al. 2007). The average grain size in these regions is approximately 0.5 mm, medium sand (-1 φ) (Nitsche et al. 2007). These average grain size data were used as reference in this study.

4. Cultural Significance of the Hudson River

The Hudson River Valley is one of the most culturally significant regions in America. In 1996 Congress established the Hudson River Valley National Heritage Area. The National Park Service website (NPS 2009) defines a National Heritage area as:

> "a place designated by the United States Congress where natural, cultural, historic and recreational resources combine to form a cohesive, nationally-distinctive landscape arising from patterns of human activity shaped by geography. These areas tell nationally important stories about our nation and are representative of the national experience through both the physical features that remain and the traditions that have evolved within them."

The Hudson River Valley National Heritage Area is one of 40 National Heritage areas (NPS 2009).

The Hudson River was discovered by Henry Hudson in 1609, and since then it has had a continuous role in the settlement of America (Doig 2001), in war and peace, facilitating both transportation and trade (Diamant 2004; Doig 2001). The analysis of short term changes around historic features on the river bed can offer a better understanding of sedimentation patterns and aid in the further identification of cultural resources such as shipwrecks or now lost defense structures.

5. Previous Research

5.a. Acoustic Sounding Techniques

Acoustic soundings are used to determine accurate water depths efficiently. Acoustic depth measurements are collected by sending a sound wave out of a transducer. When the signal returns the time taken is recorded. Based on the time taken, the angle of return, and the speed of sound waves in water, the researcher can determine the depth of the seafloor at particular locations.

As multi-beam systems have developed, more data are collected as the transducer sends out a single pulse and records an array of return signals to measure the bathymetry. With the larger amounts of data; larger processing software and hardware systems are needed to manage the data and determine depths and other associated information. Once depths are determined they are referenced to the NAV83 horizontal and NAVD88 vertical datums. After referencing the sounding data, xyz values can be plotted and geo-referenced using GIS software.

Acoustic soundings serve two important purposes: to determine depths and to identify benthic characteristics. The acoustic signals received during surveys are processed for depths (time of return) and to determine the

sediments and benthic habitats (Nitsche et al. 2004). A surface with high porosity will return a weaker signal as more energy is absorbed and the strength of the signal is attenuated whereas a surface with low porosity or strong reflectors, such as shells, will return a strong acoustic signal because more energy is scattered (Nitsche et al. 2004).

5.b. Hudson River

Hudson River estuary studies have been reported from many disciplines: archeological, geological, biological, social, and physical (Diamant, 2004; Donnelly et al. 2005; Cooper et al. 1988; Geyer et al. 2006). However, a short term temporal sediment evolution/morphological change study has not been completed.

The Hudson River Benthic Mapping Project data collected from 1998 to 2003 and was supported by NYSDEC. These surveys have resulted in several publications such as Nitsche et al. (2004) and Carbotte et al. (2004). Carbotte et al. (2004) utilized geophysical data to identify environmental changes in the Hudson River. Their study focused on oyster colonization in the Hudson River. Both surface and sub-surface geophysical data were utilized to identify present and paleo-oyster colonies. Investigations of these locations offered

documented environmental changes in the river over the past 1,000 years (Carbotte et al. 2004).

In 2005 ultra-high resolution multi-beam surveys of the Hudson River, supported by NOAA, were conducted using a Reson 8125 multi-beam survey system. These surveys added further knowledge of regions of archeological value, such as in the Hudson Highlands, and tried to identify Revolutionary War artifacts (Flood 2009, personal communication). As a result of these studies (the initial Hudson River Benthic Mapping Project and the NOAA Office of Exploration study) numerous finds of both archeological and cultural significance have been made. The significant cultural values of these artifacts confirm the importance of the studies: Shipwrecks, dredged sediments, anchor drags, and even Revolutionary War barriers are believed to have been detected. Divers have since confirmed the existence, condition, and significance of several of these artifacts. These multi-disciplinary studies have resulted in significant press for the project (e.g., New York Times 2002).

5.c. Sand Wave Migration

The properties of sand waves, their wavelength, amplitude, and shape, are dependent on current velocity, grain size, and water depth (Xu et al. 2008;

Rubin and McCulloch, 1980; Ashley 1990; Francken et al. 2004; Bartholdy et al. 2005). With expectations of such relationships between grain size, water depth and current velocity, researchers have empirical identified relationships between these variables and successfully modeled sand wave behavior and morphologies (e.g. Allen 1980; van Rijn 1984). However, what are the normally accepted theoretical (mathematical) relationships between such factors are not always able to predict natural sand wave systems in particular rivers due to factors such as the river's complicated hydrodynamics, sediment supply, antecedent morphology, and prior current velocity conditions (Whitmeyer and FitzGerald 2008).

New advancements in survey techniques with increased resolution have allowed later researchers to study temporal changes in sand waves when repeated surveys are executed (Xu et al. 2008; Weinberg and Hebbeln 2005; Ernsten et al. 2005; Barnard et al. 2006; Ernsten et al. 2006). Sand wave migration rates are difficult to quantify (Xu et al. 2008). Observed sand wave migration rates in estuarine environments range from no migration in Moriches Inlet, NY (Whitmeyer and FitzGerald 2008) up to nearly 100 m/year in Devon Estuary, United Kingdom (Masselink et al. 2009).

Using acoustic techniques, such as echosounders (Carling et al. 2000; Bartholdy et al. 2002; Dinehart 2002; Besio et al. 2008) side scan sonar

(Flemming 1978), and multi-beam bathymetry equipment (Diesing et al. 2006) researchers have found that the rate of which the sand waves migrate, although highly variable as noted immediately above, is typically on the order of ten's of meters per year (Besio et al 2004; Bokuniewicz et al. 1977; Fenster et al. 1990; Masselink et al. 2009). However, in particular estuary environments the identification of migration rates is further complicated by changing migration directions (Bartholomä et al. 2008). Due to such difficulties, and others such as variations in seasonal flow, the quality of migration rate estimates and interpretation of sand wave field behavior has to be evaluated in light of the quality and accuracy of the data available (Bartholomä et al. 2008).

In estuarine environments, sand waves often form in fine-medium sands when flow velocities are between 0.5-1.0 m/s $^{-1}$ (Masselink et al. 2009; Ashley, 1990). Sand wave migration has been recorded under conditions when current velocities exceeded 60 cm/s by Boothroyd and Hubbard (1974). To determine the rates of migration and to predict future behaviors of sand wave fields and their pattern,, repeated high accuracy surveys are needed (Masselink et al. 2009; Bates and Oakley 2004). Given the horizontal uncertainties of most marine surveys, it is difficult to precisely identify the rate of small scale migration (Whitmeyer and FitzGerald 2008). Careful

analysis of the morphology is necessary. Sometimes the best one can do is put limits (or error bars) on the measured rates.

5.d. Short Term Geomorphic Change Studies

Multi-beam imaging systems have improved in recent years (McAdoo et al. 2000; Greene et al. 2002; Smith et al. 2005; Barnard et al. 2006; Smith et al. 2007). These advancements allow the identification of small objects in the survey areas. However, studies of temporal change are still evolving (Smith et al. 2007). A recent study in the Monterey Canyon documented 29 months of change in the Canyon but results were characterized by a large range of uncertainty. For example, when estimating the volume of sedimentary flux in the Monterey Canyon 10^6 $m^3 \pm 0.7 \times 10^6$ m^3 (±70%) in 29 months was observed (Smith et al. 2007).

The resolution of short term accretion or erosion rates is also difficult. Present systems are best utilized for large scale changes in high flow conditions or in areas of extensive erosion (Smith et al. 2007). However, sand wave migration can be documented with the observation of changing patterns (Smith et al. 2005; Smith et al. 2007) and it has been expected that horizontal

changes of more than 1-3 m and vertical changes greater than 30 cm could be resolved between successive surveys (Smith et al. 2007).

6. Research Methods:

Bathymetric surveys were collected in the Lower Hudson River from 1998 to 2003 and in 2005, aboard the RV Onrust, RV Prichard and RV Seawolf (Figure 2). The 1998 to 2003 study used a Simrad EM3000 and the 2005 survey used a Reson 8125 multi-beam bathymetric survey system. Both surveys simultaneously collected vessel position information using DGPS. After collection of the 1998 to 2003 data, the Hudson River Benthic Mapping Program researchers at SoMAS mapped the data into 1 m gridded mosaics. The data collected in 2005 using the Reson 8125 was processed and mapped by SoMAS.

The 2005 Hudson River survey data were merged and edited using CARIS HIPS 6.1 survey data management and processing software. This software merged all of the sensor and tide (water elevation) information. Next, the survey lines were edited both through automatic filters and manually, line by line, to remove erroneous data. Automatic filters removed data with a slope exceeding 30 degrees which included most large spikes. Manual editing removed remaining spikes or other artifacts. Data that were deemed 'bad' were flagged as rejected and were not used in the morphological mapping of this study. Accepted data were referenced to NAVD 1988 Hudson River tidally influenced water elevation data and then

transferred into an xyz grid using 1m depth averaged gridded cells. They were finally exported as an ASCII file.

After these xyz data were exported they were imported into a 1 m grid in GIS. After initial plotting the files were converted into sun-illuminated raster images referenced to NAD83 and the vertical datum NAVD 1988. The 1 m grid was chosen because the maps created for the 1998 to 2003 data were plotted on 1 m grids. The 1 m grids also permitted the resolution of sand waves, and other small features, which may not have been resolved using a larger grid size.

These maps were then manipulated in GIS. Subtraction of the two data sets was used to identify the regions of change. Color coding was used to record where changes exceeded 30 cm between the two surveys. Depth changes greater than 30 cm indicated large changes in morphology, and areas where additional analysis would be needed.

Different types of maps were analyzed, such as bathymetry, contour lines, difference plots, and sun illuminated bathymetry images. These maps were examined for further analysis. These surveys were compared visually by analyzing the old versus new sun illuminated images, by inspecting the difference files, and by comparing horizontal profile transects to document changes in slope and bedform migration.

The locations where change greater than 30 cm occurred were identified and the transect profiles were graphed to quantify the full scope of the change. Additionally, the sand wave fields were compared and presented using sun illuminated images to identify the extent of the migration or evolution of the sand waves between 1998 to 2003 and 2005. Other examples of change identified in this way include, anchor drags, large mounds, and shipwreck evolution.

6.a. Bathymetric Data Reduction:

Multiple corrections were applied after the collection of the multi-beam data. Recorded information included the location, the orientation and position of the boat in the water (heading, roll, pitch and heave) and the sound velocity structure of the water column. Sound velocity profiles of the water column are used to correct for sound velocity variation. These profiles were collected about once every four hours during surveys. Corrections are applied to the data within the software to increase the accuracy of the morphological data.

Tidal gauge data were collected during the surveys within the survey area every 5 km in the 1998-2003 survey and at West Point and Poughkeepsie, NY using USGS tidal gauges in the 2005 survey (Figure 3). An increase in the number of tidal gauges decreases the vertical error and increases vertical

accuracy. Once USGS tide gauge data are collected they are converted from EST to GMT by adding 5 hours to all EST times, then NVGD water elevations are converted to NAVD by adding the NOAA correction of 0.267m at all stations. Once these steps are complete the files are reformatted into a CARIS HIPS tide .tid file and the water elevation at a particular time and location can be calculated. This water elevation is determined by knowing the gauge location, the vessel's distance from the gauge and how the tidal wave varies in height and amplitude along the river. Tides are a likely source of uncertainty, and determining the water level in the Hudson River is crucial since the river's tidal range is up to 2 meters. For example, if the tidal correction is off by 50 cm in 5 meters of water this would result in an error of 10%.

The 2005 survey used two USGS tidal gauges at West Point and Poughkeepsie, NY, referenced to vertical datum NGVD29, and a NOAA tidal model to estimate water elevations. Before estimates could be calculated along the Hudson River, tide (water elevation) measurements from NOAA, and the USGS were studied to determine the distance between tide zones. Tidal zones are determined so that the difference in the tide at a given point in time would not exceed 20 cm (Figures 3 and 5). This was done by using NOAA and USGS water elevation measurements and a linear model to calculate the slope of the water elevation along the river. The tidal zones were

0.025 degrees of latitude, and this distance avoided a change of water elevation of no more than 20 cm within the box. The water elevation was then calculated using USGS tidal gauges (Figure 2, Table 2).

To calculate the tide within each tide zone, the tide gauge location that is closer to the tidal zone must be identified (Figure 3). Second, the tidal offset (time) and multiplication factor from NOAA must be obtained. With this information the water elevation can be calculated using a linear model (Tables 3 and 4, Figure 4). Third, the tide gauge data must be extracted and referenced to NAVD88 for the day that is being studied. When the measurements are determined the model reads the given time, determines the true offset, reads file, applies corrections then multiplies this value by the tidal correction factor to determine the water elevation at a specific time in the tide zone (Tables 3 and 4, Figure 4).

To test if tide corrections were correct, the 1998-2003 survey was assumed to be correct, as this data had undergone extensive review and had been published by the New York State DEC. The 2005 survey data was vertically referenced using a tidal model from NOAA, and tide gauges from USGS (Figures 3-7). The tidal zones are small enough so that water elevations will not be off by more than 20 cm (Figure 3, Table 2). To test the accuracy of this model, survey lines from 2005 were compared in locations where the surveys

overlapped at different times. If the tidal model was correct, the two surveys could be expected to report similar depth readings, that is, within 20 cm. The survey data using the NOAA tidal model and USGS data produced consistent results.

6.b. System Limitations

System limitations can produce errors in spatial, horizontal placement, and depth values. The limitations can be due to imperfect vertical adjustment for the heave/squat of the vessel or due to errors in tide estimates between gauges. Sound velocity wave refraction can cause errors in bottom depths and the abilities of the equipment to interpret signals can also result in errors.

6.b.i. Horizontal System Limitations

DGPS errors can be as large as 1-2 m. If both surveys being compared have DGPS errors of less than 1 m then it is possible to observe changes less than 1 m, but when the surveys have resolutions accuracies that differ by more than 1 m it is difficult to observe actual changes (Carbotte et al. 2004). Horizontal misalignment can be identified when both sides of a feature exhibit the same horizontal shift or when a single

feature is replicated at a different depth and distance. The presence of such uncertainties requires the careful interpretation of apparent changes in water depth that can be better attributed to horizontal observation errors rather than real change.

6.b.ii. Vertical System Limitations

Major vertical errors are primarily introduced by tidal model estimates. In the 1998-2003 study tidal gauges recorded in-situ tidal measurements every 5 km up the Hudson River estuary. In the 2005 study, tidal values were calculated using NOAA time offsets and amplitude corrections and USGS tidal gauge data from West Point, NY and Poughkeepsie, NY (Figure 3). The tidal measurements in the 1998-2003 study were calculated based on closely spaced gauges and used to calculate water elevation at a particular time and location during the survey. The tidal measurements in the 2005 study were estimated using two tidal gauges which were more than 40 km apart and up to 70 km away from the survey location.

Tidal correction errors are likely in this study due to the small number of tidal gauges used in the 2005 Survey, the large distances between tide gauges, and some of the attributes of the Survey Vessel

(Figure 3). The vessel's crew attempted to limit changes in boat squat by surveying at constant speeds. Consistent survey vessel speed is essential because when the boat goes faster the boat rides lower in the water. Additionally, changing direction will change the elevation of the boat in the water. These changes are kept at a minimum to reduce errors.

6.c. Analysis:

To analyze the depth data, the 1998 to 2003 survey was subtracted from the 2005 data to produce a map of changes between the surveys. The maps used colors to display different depth changes (Figure 5). After map values had been plotted, regions of change ± 30 cm could be identified. To study these changes; profiles were produced to compare the 1998 to 2003 and the 2005 survey depth values.

Additionally, sun illuminated bathymetry maps were compared to help identify the extent of morphological change in the Hudson River (Figure 5). By toggling between the 1998 to 2003 and 2005 sun illuminated images, areas where the Hudson River bed changed considerably could be observed and investigated. Finally, in this study, sand wave migration rates were estimated by comparing wave fields with similar morphologies and measuring the

changes in the positions of sand wave crests between surveys. From these measurements, the rates of migration were estimated.

7. Results:

The 1998 to 2003 and 2005 bathymetric surveys were compared in GIS. These comparisons demonstrate morphological evolution from both natural and human factors. In particular, profiles will be presented to show morphological change. Distances reported along the profile refer to the distance along the particular profile that is being presented. Additionally, images of the sun illuminated bathymetry and change in depth between surveys will be presented. The results below provide an overview of features found throughout the Hudson River including migrating sand waves, infilling depressions, morphological changes, evidence of human disruption and systematic limitations. These observations and their importance will be discussed next.

7.a. Sand Waves

The profiles reported in Figure 5 were collected in the northern section of the Hudson River, section PN8 (Figure 1). These profiles display greater detail in 2005 perhaps due to the fact that the 2005 data used a newer higher resolution survey system [the 2005 survey used the Reson 8125 while the 2001 survey used a Simrad EM3000 system]. Also, the sediment waves

shown in Figure 5 appear to have been reworked or eroded – erosion may have smoothed the sediment waves observed in the 2001 survey.

The second observation is that the sediment waves have changed in position between surveys. While wavelengths of the sand waves remained similar between surveys (average 16 m in 2001 vs. average 18 m in 2005 wavelengths), in both surveys the sand waves appear to be asymmetric: the southwest face of the sand waves is steeper than the northern face. This wave profile indicates that the sand waves are migrating towards the southwest and this is also confirmed by comparison with the sun illuminated imagery. Because the shape of the sand waves remains similar between surveys, it is likely that these sand waves have not migrated more than 1 wavelength between surveys.

Other river sand waves have migrated 20 m ±3 m between 2001 and 2005, for example at 25 m (along the profile) the trough moved in the 2001 survey and is now a crest in the 2005 survey. The migration rate reported here has been calculated by dividing the distance that the sand wave crests have moved by the number of years between surveys-in this instance, between 2001 and 2005, 20 m divided by 4 years provides a migration rate of approximately 5 m/year southwest. Given a likely maximum horizontal uncertainty of ±3 m,

and a vertical uncertainty of ±30 cm it appears that these bed forms have changed position since the first survey.

The profiles in Figure 6 were collected in section PN8 (Figure 1). 15 m wavelengths were observed in both the 2001 and 2005 surveys. The steeper slopes of the sand waves face south suggesting that the sand waves are migrating south. Since the locations of the crests and troughs have shifted 20 m ±3 m between surveys, a migration of 5 m/year to the south has been observed. This shift in crests and troughs is visible between 90-100 m in Figure 6 where the 2005 survey shows a crest and the 1998-2003 profile displays a trough. Sand wave migration suggests, therefore, that the morphology in this location is dynamic.

The profiles in Figure 7 were collected in the northern section of the Hudson River, section PN7 (Figure 1). Both surveys show sand waves with an average wavelength of 18 m. This section of the river is dominated by fluvial sands. The steep southwest slopes of the bedforms, as shown at 50 m in Figure 7, indicates that the sand waves are migrating southwest. Between the 2001 and 2005 crests, the location of the troughs has changed. This shift in crests and trough locations is clear at 20 m in Figure 7: the 2005 survey shows a crest at 20 m and the 2001 survey shows a trough. These profiles indicate an

average migration rate of 2 m/year to the southwest suggesting a dynamic sedimentary environment.

The profiles in Figure 8 are from the northern section of the Hudson River, section PN7 (Figure 1). This profile shows that this region has a field of sediment waves. Additionally, it shows that the sand wave crests and troughs of the 2005 survey are in different locations to those reported by the 2001 survey. These features can be observed in the Figure 8 profiles between 10-30 m, and at 70 m. The steep slopes on the southwest side of these sand waves also suggest a southwest migration. The number of crests and troughs in both surveys is similar in both 2001 and 2005 as both show 20 m average wavelengths. At this location, the southwest migration of sand waves between 8 m ±3 m and 20 m ±3 m and between 2001 and 2005 indicates a 2-5 m/year migration rate. This set of observations, also suggest a dynamic morphology.

The sand wave profiles in Figure 9 were collected in the PN6 section of the Hudson River survey (Figure 1). Waves in both surveys have wavelengths of 30 m. However, the locations of the troughs and crests change between 1998 and 2005 as shown at 15 m, 50 m, 80-90 m, 110 m and 150 m in Figure 9. These sand waves appear to have migrated approximately 3m/year with a range of 10-30 m change in crest location between the 1998 and 2005 surveys. The steep slope on the southern side of the sand waves indicates southward

migration. These changes in the sand wave patterns also suggest that these features are dynamic.

The two isolated 18 meter wavelength sediment ridges in Figure 10 were identified in the PN4 area (Figure 1). The two ridges are isolated features that were resolved in both data sets. However, the crests and troughs between the initial 1998 survey and the 2005 survey have shifted 5-10 m. This shift is in excess of the horizontal ±3 meter maximum accuracy of the collection equipment, an observation suggesting that these two isolated ridges have migrated at a rate between 1-2 m/year to the southeast. It appears that the two ridges have the same morphology between surveys although they have migrated 5-10 m during the past decade. Again, these observations indicate a dynamic environment.

The images of sun illuminated bathymetry in Figure 11 were collected in the southern section of the survey area, near Yonkers in section WS6 (Figure 1). The sediment waves here did not noticeably change between 2003 and 2005 surveys. This is evident when the new 2005 sun illuminated bathymetry is compared to the 2003 image. It appears that the bed forms have not migrated between these surveys. This could be because of the short amount of time (2 years) between these two surveys or because the bed form is stable.

The sun illuminated images in Figure 12 occur near Yonkers in section WS6 (Figure 1). Here small scale asymmetrical sand waves appear to be the same in each of the 2003 and 2005 surveys. This result possibly suggests that these bed forms are only dynamic during very high energy events or, alternatively, that there has been too little time between surveys to document any migration or, that these bed-form features are permanent.

The profiles in Figure 13 are from the southern section of the survey area, section WS7 (Figure 1). This region had large rimmed-shaped depressions in the south and sediment waves in the north that exhibited a 3-6 m northward movement between the 2003 and 2005 surveys – that is, a 1.5-3.0 m/year migration rate. The average wavelength between surveys remains constant at approximately 19 m. Given the southern location, tidal forces or even meteorological events, such as floods and storm surges, could explain the sediment mobilization northward.

7.b. Depressions

The profiles from 2001 and 2005 in Figure 14 were collected in the northern section of the survey area, in section PN8 (Figure 1). These profiles cross a depression at the edge of a survey. The depression has become deeper between surveys. Although the difference is less than 1 m between the two

surveys, the general morphology of the protrusion observed in 2001 has become a larger depression between 30 m and 45 m. Both sides of the depression have become deeper and wider. If this was due to a horizontal offset alone only, one side of the depression would have been deeper. In this profile, both sides of the depression have widened between 0-25 m (distance along the profile). This suggests that the observed deepening of the hole is real and that erosion is occurring in this region.

The profiles from 1999 and 2005 in Figure 15 were collected in a depression in the northern section of the survey, area PN6 (Figure 1). The deep depression appears to have filled in as the change in depth between the two surveys exceeds 1 m based on the cross sectional profile. The shapes of the two profiles appear to be similar except for a more pronounced ½ m depression at 40 m. This area may be an area where sediment is accumulating and filling the depression.

The profiles from 2003 and 2005 in Figure 16 were collected from the PN4 region in the Hudson River (Figure 1). At 23 m, 37 m, and 40 m the morphology and bed forms changed. They exhibit deposition, and protrusion. These protrusions are pronounced and exhibit almost 1 m of change between surveys. Since the slope of the hill is not steep it is hardly plausible that sediment could slide down the slip face in this location. The origin of the

protrusions are unclear however. These regions may also be areas of no change where a ±1 to 3 m horizontal error is causing a large vertical error.

7.c. Anthropogenic Features

7.c.i. Protrusions

The images from 2001 and 2005 in Figure 17 were collected from the PN8 northern section of the survey area (Figure 1). The feature, a likely shipwreck appears to have altered sedimentation patterns. Most of the profile displays no change exceeding 0.3 vertical meters, except between 30-40 m where it appears that the sediment has accumulated on the northern (upstream) side of the feature; again, however, this observation could be the consequence of a 1 to 3 m horizontal error that is causing a large vertical error at this steeply profiled location. The morphology of the shipwreck feature also changes as its flat top has become slightly larger by the time of the 2005 survey. This set of observations display how human debris can alter sedimentation patterns in the Hudson River.

The profiles from 2001 and 2005 in Figure 18 were collected in the PN6 area (Figure 1). This is a profile across a possible shipwreck feature. The

general cross section of the shipwreck should not have changed between the 2001 and 2005 surveys. However, there is one section at 3 m where the 2005 profile is deeper than the 2001 profile. The old profile has a sharp corner, this corner may have been moved, destroyed or eroded between surveys or it could be the result of a horizontal offset between surveys, or alternatively, simply be a false profile change due to the newer high resolution Reson survey equipment used in the 2005 survey. This profile shows two features: the horizontal shift and the possible erosion of a sharp feature at 3 m.

The profiles from 2003 and 2005 in Figure 19 cross a protruding shipwreck feature in the PN3 section of the survey area (Figure 1). This feature shows the limitations of the data as the protrusion appears to have shifted approximately 3 m to the left. The horizontal shift matches the limitations of survey comparisons. It appears that change has occurred in this profile because the depression, at 17 m along the profile, has become deeper. A lip, at 19 m along the profile, appears in the 2005 survey but not the 2003 survey. These changes between the surveys appear to be based on morphologic change.

The profiles from 2003 and 2005 in Figure 20 were collected near Poughkeepsie NY in section PN1 (Figure 1). These profiles display two features, a pipe, and a bridge footing and the morphology around these

features. The first feature, the pipe at 30 m, appears to remain the same in both surveys; however, a slight survey error (or uncertainty) resulted in an apparent horizontal shift as the pipe seems to have exhibited a (false) northward migration. The second feature, the mound near the bridge base, appears to show sediment accumulation on the upstream side or is, again, perhaps evidence of horizontal error which has in its turn produced a vertical error as shown at 255 m in Figure 20. This said, sand accumulation upstream is a plausible explanation since the location is influenced by fluvial inputs.

7.c.ii. New Mounds

The profiles from 2003 and 2005 in Figure 21 were taken at West Point in Section WO (Figure 1). This section shows the largest change between surveys. In this location the area is nearly flat in the 2003 survey and, then, when the area was resurveyed the flat area shows significant relief. The relief that appears is in the shape of a large mound 3 m high, 50 m wide and 80 m long. This mound occurs between 45 m and 135 m on the profile of Figure 21. Because the profile shows that the river depth has decreased by more than 4 meters, it is clear that some sedimentary material was deposited here.

This mound represents approximately 12,000 cubic meters of new material. The isolated nature of this deposit suggests that it was of human

origin and not a natural river feature. A possible source for this material could be a barge. A typical barge on the Hudson is 100 m x 50 m and loaded with material 2-4 m high. If such a barge had dropped its load in this location it would have formed a mound of approximately this size. This mound is, therefore, probably another example of human influence on the riverbed and documents the large impact human action can have on Hudson River morphology and its benthic habitats.

The profiles from 2003 and 2005 in Figure 22 were collected near Yonkers, NY, in section WS7 (Figure 1). This shows a section where a depression has become a mound. The mound may have migrated from the mound in the 2003 profile at 7 m distance in Figure 22. However, the overall morphology appears to exhibit more sharp features than any other nearby features in the 2003 survey. A likely explanation for this unusual observation could be a difference in resolution between the survey systems; perhaps, the higher resolution Reson 8125 from the 2005 survey was able to resolve this feature while the Simrad EM3000 system used in the 2003 survey was not.

The profiles from 2003 and 2005 in Figure 23 were collected North of Poughkeepsie in section PN2 (Figure 1). These profiles show a region that is sloping towards the northwest. The protrusion feature in the older 2003 data set at 63 m appears to have been eroded and or moved towards the SE. A new

more pronounced mound feature has formed between 30-35 m. Since the less steep slope occurs at 40-50 m when compared to 20-30 m in the new PN6 profile it appears that sediment is coming from the NW and that this feature is moving to the southeast as they are moving in the same direction.

7.c.iii. Anchor Drag

The profiles from 2003 and 2005 in Figure 24 were collected south of Poughkeepsie in the PS1 section (Figure 1). This profile shows an anchor drag along the river bed. The areas adjacent to the anchor drag have filled in about 10 cm in a 20 cm anchor drag, as shown at 7 m on the profile. The morphology of the anchor drag has also changed between the two surveys, the slopes of the erosion (on the profile) are less sharp in the new survey as the feature has been smoothed, filled in, and is less pronounced in Figure 24 at 6-8 m. These profiles display yet another one way that humans have a direct effect on the morphology of the Hudson River.

7.d. Systematic/Survey Errors/Observations

The profiles from 2003 and 2005 in Figure 25 are from the Poughkeepsie region, area PO, and show both shift and a small sediment accretion. Most of

the area in this mound is unchanged. However, the difference between surveys approaches 1 m at 20 m -30 m and also from 37-40 m. These areas may be exhibiting some accretion between the 2003 and the 2005 surveys, but there is associated horizontal uncertainty. In terms of morphology, most shapes between the two surveys are similar; only at 15-20 m is there a significant alteration of the slope between the 2003 and 2005 profiles. The 2005 data set this reveals first an example of a man made feature (mound) and, second, sediment waves that do not change. Additionally, it appears that the slope here is steeper than observed earlier. At 8 m there is a second undulation or bump which was not present in the initial 2003 survey.

8. Discussion of Results

The results from the survey include three major findings. (1) The northern and southern section of the survey area experiencing dynamic change (Figures 5-13). (2) Human effects, such as shipwrecks (Figures 17-19), dredge spoils (Figures 21-23), and anchor drags (Figure 24) can produce measurable changes in river floor bathymetry. (3) Tidal corrections could be a large source of error in this study and it is clear that additional tidal measurements during surveys would increase accuracy and confidence in the survey data and the results of analysis.

8.a. Sand Waves

Consistent with data presented in Nitsche et al. 2004, the northern section of the survey area contained fluvial derived sandy sediments, and the southern section contained marine sands (Figures 5-12). The sediment waves are assumed to be made of sand since previous surveys such as Nitsche et al. (2004) describe these regions as sandy. In the central section of the survey area, bedforms were sparse if existing at all. In the northern and southern sections the profiles provide evidence that the bedforms actively moved between 1998 to 2003 and 2005 (Figures 5-13). The crests and troughs of the observed sand waves appeared to have migrated between 1-5 m/year between

surveys since their morphologies remained similar although they were found in a new location that was more than 3 m from their earlier positions (Figures 5-13). The conditions needed to initiate this movement will be discussed below.

As shown in the results section, sand waves within the survey area showed migration rates from 1 m/year to 5 m/year. In such river locations, the critical velocity needed to cause sediment movement appears to have been reached on some occasions. In the regions that exhibited migration it appears likely that strong tidal currents, for example, during spring tide events, are sufficient to cause sands wave migration. The conditions needed to initiate migration will be discussed in light of the Van Rijn equations.

The critical velocity needed to initiate sediment transport can be estimated using the Van Rijn equation (Van Rijn 1984). Sand mobilization occurs when the critical velocity is reached. Critical velocity is dependent on the grain size and sorting of the sand (Whitmeyer and FitzGerald 2008; Van Rijn 1984). The Van Rijn equation below describes the conditions needed to initiate sediment movement.

$$\overline{U_{cr}} = 0.19(d_{50})^{0.1}\log\left(\frac{4h}{d_{90}}\right) \text{for } 0.1 \text{ mm} \leq d_{50} \leq 0.5 \text{ mm}$$

$$\overline{U_{cr}} = 8.5(d_{50})^{0.6}\log\left(\frac{4h}{d_{90}}\right) \text{for } 0.5 \text{ mm} \leq d_{50} \leq 2 \text{ mm}$$

In this equation $\overline{U}_{cr}$ is the critical velocity needed to initiate sediment movement in meters per second, d_{50} is the median grain size in meters, d_{90} is the grain size in meters where 90% of the sand is finer than that value and h is the water depth in meters (Whitmeyer and FitzGerald 2008, Van Rijn 1984).

To estimate the critical velocity in the Hudson River, three different sediment sizes and four water depths were input to the Van Rijn equations under a variety of conditions -- explicitly. 0.25, 0.5, and 1.0 mm sized sediment which corresponds to fine-very fine, fine-medium, and medium-course sized sand (or phi sizes 2, 1, and 0 respectively). These were input into the Van Rijn equation with a d_{90} of 10% greater than the d_{50} at depths of 5 m, 10 m, 15 m, and 20 m and used to estimate the critical velocities (Figure 26). These specifications and the Van Rijn equations indicate that in the Hudson River the critical velocities at the bed of between 0.4-0.66 meters/second are needed to initiate sand movement (Figure 26). Once movement has been initiated lower velocities can be sufficient to sustain sedimentary movement and sand wave migration.

The estimates for critical velocity reported above were compared to recent Hudson River current velocity data to establish whether typical tidal currents could initiate sediment transport. A recent study by Trowbridge et al. (1999) recorded mean velocity ebb and flood currents of 0.2 m/s 50 cm above the sediment water interface ≈10 km north of the Battery in the Fall of 1995. A

more recent study by Geyer et al. (2001) recorded near bed tidal current velocity maximum amplitudes ranging from 0.5-0.85 m/s less than 10 km north of the Battery during the spring of 1999. Geyer et al. (2001) indicate that the monthly maxima in current velocities occur during spring tides and that these events are likely to be the most influential with regards to sediment transport and sand wave migration.

Near bed current velocity estimates ranging from 0.2 m/s- 0.85 m/s were collected just north of the Battery, NY. The largest magnitude tidal currents in the Hudson River have been recorded at this location (DiLorenzo et al. 1999). These values will be adopted here as likely maximum velocities within the Hudson River estuary. Of course, these recorded current velocities only offer a snap shot of possible higher energy events that may not have been recorded in earlier research studies.

Based on the data incorporated into this study, the observed sand wave migrations in the northern and southern sections of the Hudson River could be explained by monthly maximum tidal currents of greater than 0.4 -0.66 m/s. Additionally, to initiate sediment movement where residual ebb and flood tidal flows are insufficient, major meteorological events, like a storm surges or floods, may initiate movement on a decadal scale, if not longer. Such findings were reported for Moriches Inlet by Whitmeyer and FitzGerald (2008), yet during their repeated surveys no sand wave migration was

observed due to lack of strong currents. As a consequence, Whitmeyer and FitzGerald (2008) suggested that even spring tides did not produce strong enough currents to initiate sand wave migration at Moriches. This led them to conclude that it was probable that only during strong tides which were compounded by meteorological forces (storm surge) could strong enough currents occur to cause sand wave migration.

However, this study which has recorded sand wave migration in the Hudson at multiple locations indicates that spring tides and their associated current velocities are strong enough to have caused sand wave migration in, at least, some locations in the Hudson River.

8.b. Anthropogenic Effects

Throughout the study area, examples of human impact on river bed bathymetry were evident. These impacts consisted of such features as shipwrecks (Figures 17-19), ship-derived deposits (possible dredged sediments or other debris (Figures 21-23) and anchor drags (Figure 24). These features can alter, not only the shape of the river floor, but also the benthic habitats that they disturb.

Shipwrecks are visible and present throughout the Hudson River. These shipwrecks leave a distinct impression on the river floor (Figure17-19). Sedimentation patterns also shift due to these features. Most notably sediment appears to accumulate on the upstream side of the shipwrecks; this observation is evident in Figure 17. The sediment likely is not able to move around the shipwreck and is trapped and accumulates. Shipwrecks because of their size and sedimentation influence must also alter benthic habitats.

The largest example of human influence observed in this survey was a new mound found in section WO (Figure 21) near West Point. Here, in section WO, a large mound appeared in the 2005 survey which was not present in the 2003 survey (Figure 21). The large size of this feature and its shape suggests that a matched sized barge probably likely dumped sedimentary material in this location. The newly deposited (or dumped) material likely changed benthic communities, and altered the sediment characteristics of the River nearby.

Other human impacts on the riverbed were anchor drag marks that were observed in many places within the survey area (Figure 24). These anchor drags may be the product of boats trying to remain stationary in the river, or the result of anchors deployed by accident as ships or barges pass up or down river. As these events occur, anchors dig into the sediment and make a large impact because these features are easily identifiable in bathymetric surveys.

Additionally, these anchor drags likely disrupt benthic habitats and clearly take much longer to restore than they do to create.

9. Future Work:

To improve the accuracy and utility of short term bathymetric comparisons, numerous changes could be implemented. Over time repetitive surveys over tidal cycles, week by week, or month by month, or seasonally, would allow sedimentary changes to be more readily identified. To reduce error in the data sets improved mapping equipment and techniques could be deployed. Finally, more tidal gauges are a necessity -- ideally sufficient tide gauges should have been installed for the 2005 survey to allow more exact comparisons with the 1998-2003 surveys (which had numerous tidal gauges). Also, the use of newer RTK GPS positioning systems would increase accuracy when compared to the GPS or DGPS systems used in the surveys referenced here (Hu et al. 2003). These improvements would reduce error, and so improve accuracy and facilitate interpretation.

10. Conclusion:

This study confirms that multiyear temporal morphological change occurs in rivers such as the Hudson and that such change can be identified using multi-beam sonar systems. The comparisons made here revealed dynamic sedimentary environments in the northern and southern section of the Hudson River survey areas probably due to regular spring tidal currents. These comparisons also revealed the morphological impact, and likely benthic impact, of human actions, such as anchor drags, or dumpings. The limitations of survey to survey comparisons were revealed and tested during this study.

To minimize error more accurate equipment would help. With such equipment, and using proven but identical collection techniques and data processing steps, we would advance our understanding of short term morphological effects. This includes both evolutionary processes such as sand wave behavior and human impacts on the local morphology of rivers such as the Hudson.

References:

Abood K.A.; 1974; Circulation in the Hudson River; Annals of the New York Academy of Sciences 250; 39-111.

Allen J.R.L.; 1980; Sand waves: a model of origin and internal structure; Sedimentary Geology 26; pp. 281–328.

Ashley G.M.; 1990, Classification of large-scale subaqueous bedforms: a new look at an old problem; Journal of. Sedimentary Petroleum 60; pp. 160–172

Barnard P.L., Hanes D.M., Rubin, D.M., Kvitek, R.G.; 2006; Giant sand waves at the mouth of San Francisco Bay; Eos 87; pp 285–289

Bartholdy J., Flemming B.W., Bartholoma A. and Ernstsen V.B.; 2005; Flow and grain size control of depth-independent simple subaqueous dunes; Journal of Geophysical Research 110; F04S16

Bartholdy J., Bartholomae A. and Flemming B.W.; 2002; Grainsize control of large compound flow-transverse bedforms in a tidal inlet of the Danish Wadden; Marine Geology 188; pp. 391–413

Bartholomä A, Schrottke K, Winter C.; 2008; Sand wave dynamics: Surfing between assumptions and facts; In: Parsons D, Garlan T, Best J (eds) Marine and River Dune Dynamics; pp. 17–24

Bates C.R. and Oakley D.J.; 2004; Bathymetric sidescan investigation of sedimentary features in the Tay Estuary, Scotland; International Journal of Remote Sensing 25; pp. 5089–5104

Bell R.E., Flood R.D., Carbotte S.M., Ryan W.B.F., McHugh C.M.G., Cormier M., Versteeg R., Bokuniewicz H., Ferrini V., Thissen J.; 2000; Hudson River Estuary Program Benthic Mapping Project. Final Report Estuary to New York: Department of Environmental Conservation

Bell R.E., Flood R.D., Carbotte S.M., Ryan W.B.F., McHugh C.M.G., Cormier M., Versteeg R., Bokuniewicz H., Ferrini V., Thissen J.; 2003; Hudson River Estuary Program Benthic Mapping Project: Final Report Estuary to New York Department of Environmental Conservation Phase II Rep 1

Besio G., Blondeaux P., Brocchini M., Hulscher S.J.M.H., Idier D., Knaapen M.A.F., Németh A.A., Roos P.C. and Vittori G.; 2008; The morphodynamics of tidal sand waves: a model overview; Coastal Engineering 55 ; pp. 657–670

Besio G., Blondeaux P., Brocchini M. and Vittori G.; 2004; On the modeling of sand wave migration; Journal of Geophysical Research Oceans 109

Bird, E.; 2000; Coastal Geomorphology- An Introduction. John Wiley and Sons; Chichester, 322 p

Boothroyd J.C. and Hubbard D.K.; 1974; Bed form development and distribution pattern, Parker and Essex Estuaries, Massachusetts, Miscellaneous Paper 1-74; U.S. Army Corps of Engineers, Coastal Engineering Research Center, Fort Belvoir, VA

Bokuniewicz H., Gordon R.B., and Kastens K.A.; 1977; Form and migration of sand waves in a large estuary, Long Island Sound; Marine Geology 24; pp. 185–199

Carling P. A., Gölz E., Orr H.G., and Radecki-Pawlik A.; 2000; The morphodynamics of fluvial sand dunes in the River Rhine near Mainz, Germany, part I: Sedimentology and morphology; Sedimentology 47; pp. 227–252

Carbotte S.M., Bell R.E., Ryan W. B. F., McHugh C., Stagle, Nitsche F.O., Rubenstone J.; 2004; Environmental change and oyster colonization within the Hudson River estuary linked to Holocene Climate; Marine Geology Letters 24; pp. 212-224

Cooper J.C., Cantemmo F.R., Newton C.E.; 1988; Overview of the Hudson River estuary; American Fish Society Monograph 4; pp. 11-24

Diamant L.; 2004; Chaining the Hudson: The Fight for the River in the American Revolution; Fordham University Press; New York

Diesing M., Kubicki A., Winter C. and Schwarzer K.; 2006; Decadal scale stability of sorted bedforms, German Bight, southeastern North Sea; Continental Shelf Research 26; pp. 902-916

Dinehart R. L.; 2002; Bedform movement recorded by sequential single-beam surveys in tidal rivers; Journal of Hydrology 258; pp. 25-39

DiLorenzo J.L., Huang P., Ulman D., and Najarian T.O.; 1999; Hydrologic and anthropogenic controls on the salinity distribution of the middle Hudson-River Estuary. Final Report prepared for the Hudson River Foundation

Darymple R.W., Zaitlin B.A., Boyd R.; 1992; Estuarine facies models; conceptual basis and stratigraphic implications; Journal of Sedimentary Petrology 62; pp. 1130-1146

Doig J.W.; 2001; Empire on the Hudson: Entrepreneurial Vision and Political Power at the Port of New York Authority; Columbia University Press, NY, NY

Donnelly J.P., Driscoll N.W., Uchupi E., Keigwin L.D., Schwab W.C., Thieler E.R. and Swift S.A.; 2005; Catastrophic meltwater discharge down the Hudson Valley: a potential trigger for the Intra-Allerod cold period; Geology 33; pp. 89–92

Ernsten V.B., Noormets R., Winter C., Hebbeln D., Bartholoma A., Flemming and J. Bartholdy B.W.; 2005; Development of subaqueos barchanoid-shaped dunes due to lateral grain size variability in a tidal inlet channel of Danish Wadden Sea, Journal of Geophysical. Research 110; F04S08

Ernsten V.B., Noormets R., Winter C., Hebbeln C., Bartholoma A., Flemming B.W. and Bartholdy J.; 2006; Quantification of dune dynamics during a tidal cycle in an inlet channel of the Danish Wadden Sea; Geologic Marine Letters 26; pp. 151–163

Fenster M. S., Fitzgerald D.M., Bohlen W.F., Lewis R.S., and Baldwin C.T.; 1990; Stability of giant sand waves in eastern Long Island Sound, U.S.A., Marine Geology 91; pp. 207– 225

Flemming B.W.; 1978; Underwater sand dunes along the southeast African continental margin - observations and implications; Marine Geology 26; pp. 177-198

Flood R; 2009; Professor of Marine Sciences; Stony Brook University; Stony Brook, NY

Francken F., Wartel S., Parker R. and Taverniers E.; 2004; Factors influencing subaqueous dunes in the Scheldt Estuary; Geologic Marine Letters; pp. 14–24

Geyer W.R, and Chant R.; 2006; The physical oceanography process in the Hudson River; In the Hudson River Estuary; eds. J.S. Levinton and J R Waldman; 24-38; New York City USA: Cambridge University Press

Geyer W.R., Trowbridge J.H. and Bowen M.M.; 2000; The dynamics of a partially mixed estuary; Journal of Physical Oceanography 30; pp. 2035-2048

Geyer W.R., Woodruff J.D. and Traykovski P.; 2001; Sediment transport and trapping in the Hudson River Estuary; Estuaries 24; pp. 670-679

Greene H.G., Maher N. and Paull C.K.; 2002; Physiography of the Monterey Bay Marine Sanctuary and implications about continental margin development; In: Ettreim, S.A., Noble, M. (Eds.), Special Issue: Seafloor Geology and Natural Environments of the Monterey Bay National Marine Sanctuary; Marine Geology 181; pp. 55–84

Hu G.R., Khoo H.S., Goh P.C. and Law C.L.; 2003; Development and assessment of GPS virtual reference stations for RTK positioning; Journal of Geodesy 77; pp. 291-302

Isachsen Y.W., Landing E., Auber J.M., Rickard L.V., Rogers W.B.; 2000; Geology of New York: a simplifies account; New State Museum Educational Leaflets 28; The New York State Geological Survey; New York State Museum, Albany, New York, USA; pp. 1-294

Masselink G., Cointre L., Williams J., Gehrels R. and Blake B.; 2009; Tide-driven dune migration and sediment transport on an intertidal shoal in a shallow estuary in Devon; UK Marine Geology 262; pp. 82-95

McAdoo B., Pratson G.L., and Orange D.L.; 2000; Submarine landslide geomorphology, US continental slope; Marine Geology 169; pp. 103-136

Menon M.G, Gibbs R.J, Phillips A; 1998; Accumulation of muds and metals in the Hudson River estuary turbidity maximum; Environmental Geology 34; pp. 214-222

(NPS) National Park Service ; 2009; http://www.nps.gov/history/heritageareas/FAQ/INDEX.HTM

Newman W.S., Thurber D.H., Zeiss H.S., Rokach and Musich L.; 1969; Late Quaternary geology of the Hudson River estuary, a preliminary report; Transactions of the New York Academy of Sciences 31; pp. 548-569

New York Times; 2002; Johnson, K; Hudson Shipwrecks Found But No Loose Lips; 12/18/2002

Nichols M.M., Biggs R.B.; 1985; Estuaries; In Davis Jr. RA Coastal Sedimentary Environments; Second Edition; Springer-Verlag, New York, pp. 77-186

Nitsche F.O., Ryan W. B. F., Carbotte S. M., Bell R. E., Slagle A, Bertinado C., Flood R., Kenna T., and McHugh C.; 2007; Regional patterns and local variations of sediment distribution in the Hudson River Estuary; Estuarine, Coastal and Shelf Science Volume 71; pp. 259-277

Nitsche F.O., Bell R.E., Carbotte S.M., Ryan W.B.F., Flood R.D., Ferrini V, Slagle A., McHugh C.M.G., Chillrud S., Kenna T., Strayer D.L., and Cerrato R.M.; 2006; Integrative acoustic mapping reveals Hudson River sediment processes and habitats; EOS Transactions, American Geophysical Union 86; pp. 225- 229

Nitsche, F.O., Bell, R., Carbotte, S.M., Ryan,W.B.F., Flood, R.; 2004; Process related classification of acoustic data from the Hudson River Estuary; Marine Geology 209; pp. 131-145

Olsen C.R., Simpson H.J., Bopp R.F., Williams S.C., Peng T.H. and Deck B.L.; 1978; A geochemical analysis of the sediments and sedimentation in the Hudson River estuary; Journal of Sedimentary Petrology 48; pp. 401-418

Peltier W.R.; 1998; Postglacial variations in the level of the sea: implications for climate dynamics and solid-earth geophysics; Reviews of Geophysics 36; pp. 603–689

Peteet D.M. and Wong J.K.; 2000; Late Holocene environmental changes from NY-NJ estuaries; Proceedings Geological Society of America Northeast Section Meeting; pp. A-65

Rubin D.M. and McCulloch D.S.; 1980; Single and superimposed bedforms: a synthesis of San Francisco Bay and flume observations, Sedimentary Geology 26; pp. 207–231

Sirkin L. and Bokuniewicz H.; 2006; The Hudson River Valley: geological history, landforms, and resources. In: J.S. Levinton and J.R. Waldman, Editors; The Hudson River Estuary; Cambridge University Press, New York, NY; pp. 13–23

Smith D., Kvitek R., Iampietro P., and Wong K.; 2007; Twenty-nine months of geomorphic change in upper-Monterey Canyon (2002-2005); Marine Geology 236; pp. 79-94

Smith D., Ruiz D., Kvitek R., and Iampietro P.; 2005; Semi-annual patterns of erosion and deposition in Upper Monterey Canyon from serial multi-beam bathymetry; Geological Society of America Bulletin; pp. 1123-113

Trowbridge J.H., Geyer W.R., Bowen M.M., and Williams III; 1999; Near-Bottom Turbulence Measurements in a Partially Mixed Estuary: Turbulent Energy Balance, Velocity Structure, and Along-Channel Momentum Balance; Journal of Physical Oceanography 29; pp. 3056-3072

Uchupi E. N., Driscoll R.D., Ballard and Bolmer S.T; 2001; Drainage of late Wisconsin glacial lakes and the morphology and late quaternary stratigraphy of the New Jersey - southern New England continental shelf and slope; Marine Geology 172; pp. 117–145

Van Rijn L.C.; 1984; Sediment transport, part I: bed load transport; Journal of Hydraulic Engineering 110; pp. 1431–1456

Water Resources Data Report; 1977; New York State. United States Geological Survey; http://water.usgs.gov/data/

Weiss; 1974; Late Pleistocene stratigraphy and Paleoecology of the Lower Hudson River Estuary; Geological Society of America Bulletin 85; pp. 1561–1570

Whitmeyer S.J. and D.M. FitzGerald D.M.; 2008; Episodic dynamics of a sand wave field; Marine Geology 252; pp. 24–37

Weinberg C. and Hebbeln D.; 2005; Impact of dumped sediments on subaqueous dunes, outer Weser Estuary, German Bight, southeastern North Sea, Geology Marine Letters 25; pp. 43–53

Xu J.P., Wong F., Kvitek R., Smith D. and. Paull C; 2008; Sandwave migration in Monterey Submarine Canyon, Central California; Marine Geology 248; pp. 193-212

Appendix 1:

Table 1: Hudson River Field Sheet box coordinates

Map Zone Box Coordinates

Field Sheet (Region)	Northeast Corner Limits	Northwest Corner	South East Corner	Southwest Corner
PN8	73°47'54.214"W 42°15'20.098"N	73°51'24.408"W 42°15'30.956"N	73°47'51.312"W 42°12'9.899"N	73°51'46.865"W 42°12'12.301"N
PN7	73°47'51.312"W 42°12'9.899"N	73°51'46.865"W 42°12'12.301"N	73°48'4"W 42°7'11.175"N	73°56'48.047"W 42°7'22.257"N
PN6	73°48'4"W 42°7'11.175"N	73°56'48.047"W 42°7'22.257"N	73°53'17.696"W 42°1'56.297"N	73°57'34.925"W 42°1'49.995"N
PN5	73°53'17.696"W 42°1'56.297"N	73°57'34.925"W 42°1'49.995"N	73°55'30.416"W 41°55'53.627"N	73°59'12.122"W 41°55'54.191"N
PN4	73°55'30.416"W 41°55'53.627"N	73°59'12.122"W 41°55'54.191"N	73°55'30.012"W 41°52'25.948"N	73°58'42.468"W 41°52'20.444"N
PN3	73°55'30.012"W 41°52'25.948"N	73°58'42.468"W 41°52'20.444"N	73°55'45.757"W 41°48'20.95"N	73°57'59.74"W 41°48'17.82"N
PN2	73°55'45.757"W 41°48'20.95"N	73°57'59.74"W 41°48'17.82"N	73°55'59.26"W 41°44'31.902"N	73°58'22.735"W 41°44'33.209"N
PN1	73°55'59.26"W 41°44'31.902"N	73°58'22.735"W 41°44'33.209"N	73°55'55.818"W 41°40'11.324"N	73°57'44.225"W 41°40'15.222"N
PO	73°55'55.818"W 41°40'11.324"N	73°57'44.225"W 41°40'15.222"N	73°56'28.85"W 41°38'6.729"N	73°57'32.75"W 41°38'5.86"N
PS1	73°56'28.85"W 41°38'6.729"N	73°57'32.75"W 41°38'5.86"N	73°56'35.555"W 41°36'17.917"N	73°57'54.796"W 41°36'15.935"N
PS2	73°56'35.555"W 41°36'17.917"N	73°57'54.796"W 41°36'15.935"N	73°56'59.123"W 41°33'38.889"N	73°58'32.261"W 41°33'38.685"N
PS3	73°56'59.123"W 41°33'38.889"N	73°58'32.261"W 41°33'38.685"N	73°57'41.551"W 41°31'26.68"N	74°0'28.323"W 41°31'22.932"N
PS4	73°57'41.551"W 41°31'26.68"N	74°0'28.323"W 41°31'22.932"N	73°59'4.64"W 41°28'1.612"N	74°1'18.106"W 41°28'10.599"N
WN2	73°59'4.64"W 41°28'1.612"N	74°1'18.106"W 41°28'10.599"N	73°58'24.547"W 41°26'23.375"N	74°1'38.692"W 41°26'30.282"N
WN1	73°58'24.547"W 41°26'23.375"N	74°1'38.692"W 41°26'30.282"N	73°56'54.471"W 41°24'29.018"N	74°0'5.232"W 41°24'24.192"N
WO	73°56'54.471"W 41°24'29.018"N	74°0'5.232"W 41°24'24.192"N	73°56'32.533"W 41°22'5.257"N	73°58'47.645"W 41°22'6.476"N
WS1	73°56'32.533"W 41°22'5.257"N	73°58'47.645"W 41°22'6.476"N	73°57'2.91"W 41°19'19.786"N	73°59'45.503"W 41°19'29.067"N
WS2	73°57'2.91"W 41°19'19.786"N	73°59'45.503"W 41°19'29.067"N	73°56'40.486"W 41°17'27.341"N	73°59'45.694"W 41°17'23.778"N
WS3	73°56'40.486"W 41°17'27.341"N	73°59'45.694"W 41°17'23.778"N	73°56'40.858"W 41°15'16.832"N	73°59'28.592"W 41°15'18.336"N
WS4	73°56'40.858"W 41°15'16.832"N	73°59'28.592"W 41°15'18.336"N	73°53'39.824"W 41°9'35.799"N	73°58'50.712"W 40°57'28.719"N
WS5	73°53'39.824"W 41°9'35.799"N	73°58'50.712"W 41°9'33.446"N	73°52'20.973"W 41°9'38.732"N	74°0'24.414"W 41°9'12.246"N
WS6	73°52'20.973"W 41°9'38.732"N	74°0'24.414"W 41°9'12.246"N	73°48'19"W 41°2'32.457"N	74°0'1.961"W 41°2'23.68"N
WS7	73°48'19"W 41°2'32.457"N	74°0'1.961"W 41°2'23.68"N	73°52'28.451"W 40°57'21.049"N	73°56'47.72"W 40°57'28.719"N
WS8	73°52'28.451"W 40°57'21.049"N	73°56'47.72"W 40°57'28.719"N	73°51'57.353"W 40°51'51.834"N	74°0'35.505"W 40°51'46.164"N

Table 2: Hudson River Tide Zone Box Coordinates

Tide Zone Box Coordinates

HR0		HR5		HR10		HR15		HR20		HR25	
N	W	N	W	N	W	N	W	N	W	N	W
38.4111	-74.25	41.4861	-74.25	41.6111	-74.25	41.7361	-74.25	41.8611	-74.25	41.9861	-74.25
38.4111	-71.75	41.4861	-73.75	41.6111	-73.75	41.7361	-73.75	41.8611	-73.75	41.9861	-73.75
41.4111	-71.75	41.5111	-73.75	41.6361	-73.75	41.7611	-73.75	41.8861	-73.75	42.0111	-73.75
41.4111	-74.25	41.5111	-74.25	41.6361	-74.25	41.7611	-74.25	41.8861	-74.25	42.0111	-74.25
38.4111	-74.25	41.4861	-74.25	41.6111	-74.25	41.7361	-74.25	41.8611	-74.25	41.9861	-74.25
HR1		HR6		HR11		HR16		HR21		HR26	
N	W	N	W	N	W	N	W	N	W	N	W
41.3861	-74.25	41.5111	-74.25	41.6361	-74.25	41.7611	-74.25	41.8861	-74.25	42.0111	-74.25
41.3861	-73.75	41.5111	-73.75	41.6361	-73.75	41.7611	-73.75	41.8861	-73.75	42.0111	-73.75
41.4111	-73.75	41.5361	-73.75	41.6611	-73.75	41.7861	-73.75	41.9111	-73.75	42.0361	-73.75
41.4111	-74.25	41.5361	-74.25	41.6611	-74.25	41.7861	-74.25	41.9111	-74.25	42.0361	-74.25
41.3861	-74.25	41.5111	-74.25	41.6361	-74.25	41.7611	-74.25	41.8861	-74.25	42.0111	-74.25
HR2		HR7		HR12		HR17		HR22		HR27	
N	W	N	W	N	W	N	W	N	W	N	W
41.4111	-74.25	41.5361	-74.25	41.6611	-74.25	41.7861	-74.25	41.9111	-74.25	42.0361	-74.25
41.4111	-73.75	41.5361	-73.75	41.6611	-73.75	41.7861	-73.75	41.9111	-73.75	42.0361	-73.75
41.4361	-73.75	41.5611	-73.75	41.6861	-73.75	41.8111	-73.75	41.9361	-73.75	42.0611	-73.75
41.4361	-74.25	41.5611	-74.25	41.6861	-74.25	41.8111	-74.25	41.9361	-74.25	42.0611	-74.25
41.4111	-74.25	41.5361	-74.25	41.6611	-74.25	41.7861	-74.25	41.9111	-74.25	42.0361	-74.25
HR3		HR8		HR13		HR18		HR23		HR28	
N	W	N	W	N	W	N	W	N	W	N	W
41.4361	-74.25	41.5611	-74.25	41.6861	-74.25	41.8111	-74.25	41.9361	-74.25	42.0611	-74.25
41.4361	-73.75	41.5611	-73.75	41.6861	-73.75	41.8111	-73.75	41.9361	-73.75	42.0611	-73.75
41.4611	-73.75	41.5861	-73.75	41.7111	-73.75	41.8361	-73.75	41.9611	-73.75	42.0861	-73.75
41.4611	-74.25	41.5861	-74.25	41.7111	-74.25	41.8361	-74.25	41.9611	-74.25	42.0861	-74.25
41.4361	-74.25	41.5611	-74.25	41.6861	-74.25	41.8111	-74.25	41.9361	-74.25	42.0611	-74.25
HR4		HR9		HR14		HR19		HR24		HR29	
N	W	N	W	N	W	N	W	N	W	N	W
41.4611	-74.25	41.5861	-74.25	41.7111	-74.25	41.8361	-74.25	41.9611	-74.25	42.0861	-74.25
41.4611	-73.75	41.5861	-73.75	41.7111	-73.75	41.8361	-73.75	41.9611	-73.75	42.0861	-72.75
41.4861	-73.75	41.6111	-73.75	41.7361	-73.75	41.8611	-73.75	41.9861	-73.75	43.0861	-72.75
41.4861	-74.25	41.6111	-74.25	41.7361	-74.25	41.8611	-74.25	41.9861	-74.25	43.0861	-74.25
41.4611	-74.25	41.5861	-74.25	41.7111	-74.25	41.8361	-74.25	41.9611	-74.25	42.0861	-74.25

Table 3: Location of USGS tide guges used in model estimates during 2005 survey, and the Specifications for each tide zone, time offset, and tide multiplication factor. Data obtained from USGS 2010 http://waterdata.usgs.gov/ny/nwis/rt

	Location of USGS Tide Gauges	
USGS Tide Station	N	W
Poughkeepsie	41.650833	-73.945
WestPoint	41.3861	-73.9555

Tide Zone Specifications			
Tide Zone	USGS Tide Reference Station	Time ofset (minutes)	Tide Multiplier
HR0	WestPoint	0	1
HR1	WestPoint	0	1.007189
HR2	WestPoint	7.409	1.014378
HR3	WestPoint	14.81818	1.021567
HR4	WestPoint	22.22727	1.028756
HR5	WestPoint	29.63636	1.035945
HR6	WestPoint	37.04545	1.043134
HR7	Poughkeepsie	-29.63636	0.96992
HR8	Poughkeepsie	-22.22727	0.976604
HR9	Poughkeepsie	-14.81818	0.983289
HR10	Poughkeepsie	-7.4	0.989973
HR11	Poughkeepsie	0	1
HR12	Poughkeepsie	7.4	1
HR13	Poughkeepsie	13.9	1.00367
HR14	Poughkeepsie	20.4	1.007353
HR15	Poughkeepsie	26.9	1.011029
HR16	Poughkeepsie	33.4	1.014706
HR17	Poughkeepsie	36.7	1.045343167
HR18	Poughkeepsie	40	1.075980333
HR19	Poughkeepsie	43.4	1.1066175
HR20	Poughkeepsie	46.7	1.137254667
HR21	Poughkeepsie	50	1.167891833
HR22	Poughkeepsie	53.3	1.198529
HR23	Poughkeepsie	58.6	1.209558
HR24	Poughkeepsie	63.8	1.220588
HR25	Poughkeepsie	69	1.231617
HR26	Poughkeepsie	72.1	1.242647
HR27	Poughkeepsie	77.3	1.253676
HR28	Poughkeepsie	82.5	1.264706
HR29	Poughkeepsie	87.7	1.264706

Table 4: Example tide data from the West Point USGS tidal gauge and the calculation results in tidal model box HR3

West Point Water Elevation Data NOAA

Date	Time	Depth (m) (Relative to NAVD88)
11/13/2005	5:00:00	-0.08839
11/13/2005	5:15:00	-0.12497
11/13/2005	5:30:00	-0.15545
11/13/2005	5:45:00	-0.19202
11/13/2005	6:00:00	-0.22555
11/13/2005	6:15:00	-0.24994
11/13/2005	6:30:00	-0.27127
11/13/2005	6:45:00	-0.28651
11/13/2005	7:00:00	-0.29261
11/13/2005	7:15:00	-0.27737

Tide Zone HR3 Water Elevation Data using Model

Time Offset (-)15 minutes Tide multiplier 1.021567

Date	Time	Depth (m) (Relative to NAVD88)
11/13/2005	5:00:00	-
11/13/2005	5:15:00	-0.0903
11/13/2005	5:30:00	-0.12766
11/13/2005	5:45:00	-0.1588
11/13/2005	6:00:00	-0.19617
11/13/2005	6:15:00	-0.23042
11/13/2005	6:30:00	-0.25533
11/13/2005	6:45:00	-0.27712
11/13/2005	7:00:00	-0.29269
11/13/2005	7:15:00	-0.29892

Appendix 2:

Figure 1: Map of the Lower Hudson River. The boxes represent the study areas and each box corresponds to a different "field map zone" used to segment the data to allow efficient processing. The base map in the figure is from Google Earth (Version 5.1.3533.1731) [Software]. Mountain View, CA: Google Inc. (2009).


Troy, NY
Hudson, Ny
PN8
PN7
PN6
PN5
PN4
PN3
PN2
PN1
PO
PS1
PS2
PS3
PS4
WN2
WN1
WO
WS1
WS2
WS3
WS4
WS5
WS6
WS7
WS8
Poughkeepsie, NY
West Point, NY
Connecticut
N
Newark
New York City, NY
100 km
The Battery, NYC
Data SIO, NOAA, U.S. Navy, NGA, GEBCO

Figure 2: Image of R/V Onrust (top), R/V Seawolf and R/V Pritchard (bottom). Images from SoMAS (http://www.somas.stonybrook.edu/facilities/research_vessels.html).

Figure 3: Map of the tide zones in the Lower Hudson River. Each zone allows the tide to be within 20 cm in all locations in each tide zone box throughout a tidal cycle. The base map in the figure is from Google Earth (Version 5.1.3533.1731) [Software]. Mountain View, CA: Google Inc. (2009).

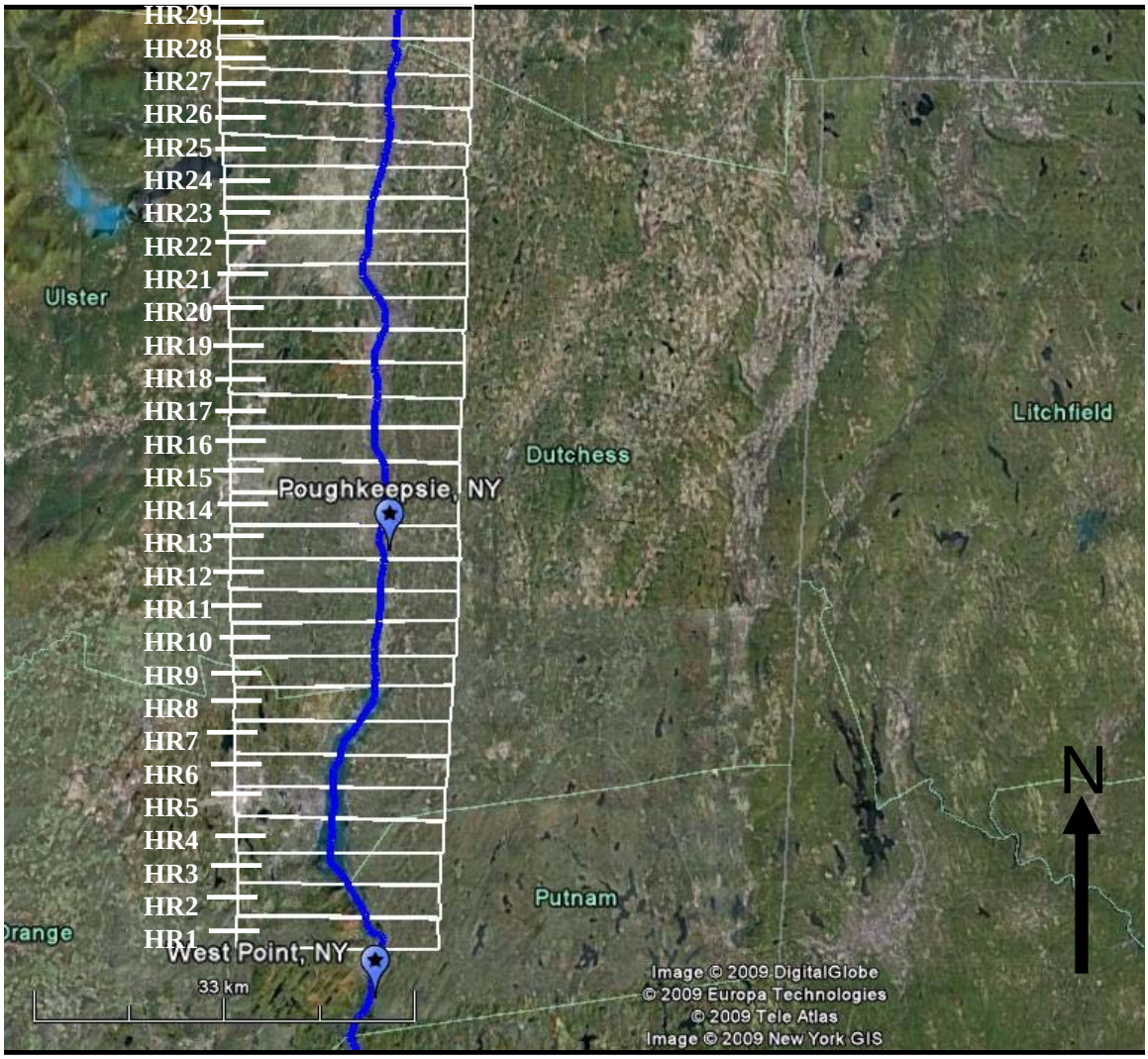
HR29
HR28
HR27
HR26
HR25
HR24
HR23
HR22
HR21
HR20
HR19
HR18
HR17
HR16
HR15
HR14
HR13
HR12
HR11
HR10
HR9
HR8
HR7
HR6
HR5
HR4
HR3
HR2
HR1
Ulster
Poughkeepsie, NY
Dutchess
Litchfield
Putnam
West Point, NY
33 km
N
Image © 2009 DigitalGlobe
© 2009 Europa Technologies
© 2009 Tele Atlas
Image © 2009 New York GIS

Figure 4: Example tide plot November 13th 2005: water elevation comparison between West Point tide gauge results and HR3 tide zone calculations using NOAA water elevation models. HR3 is 15 km north of the West Point tide gauge.

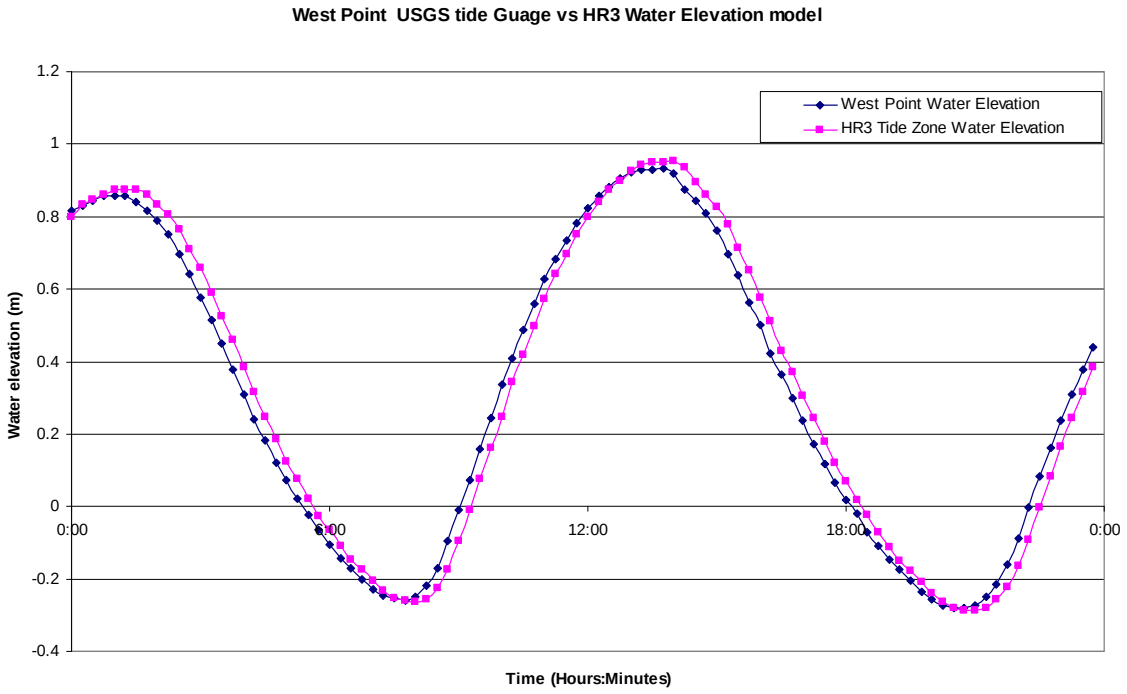

November 13th 2005

Figure 5: The map shows the difference in depth between 2001 and 2005 surveys. This depth difference is plotted on top of the sun illuminated bathymetry of the 2001 survey in section PN8.

The graph below shows the depth profile from A-B, the blue line is the depth during the 2005 survey and the pink line is the depth data from the 2001 survey.

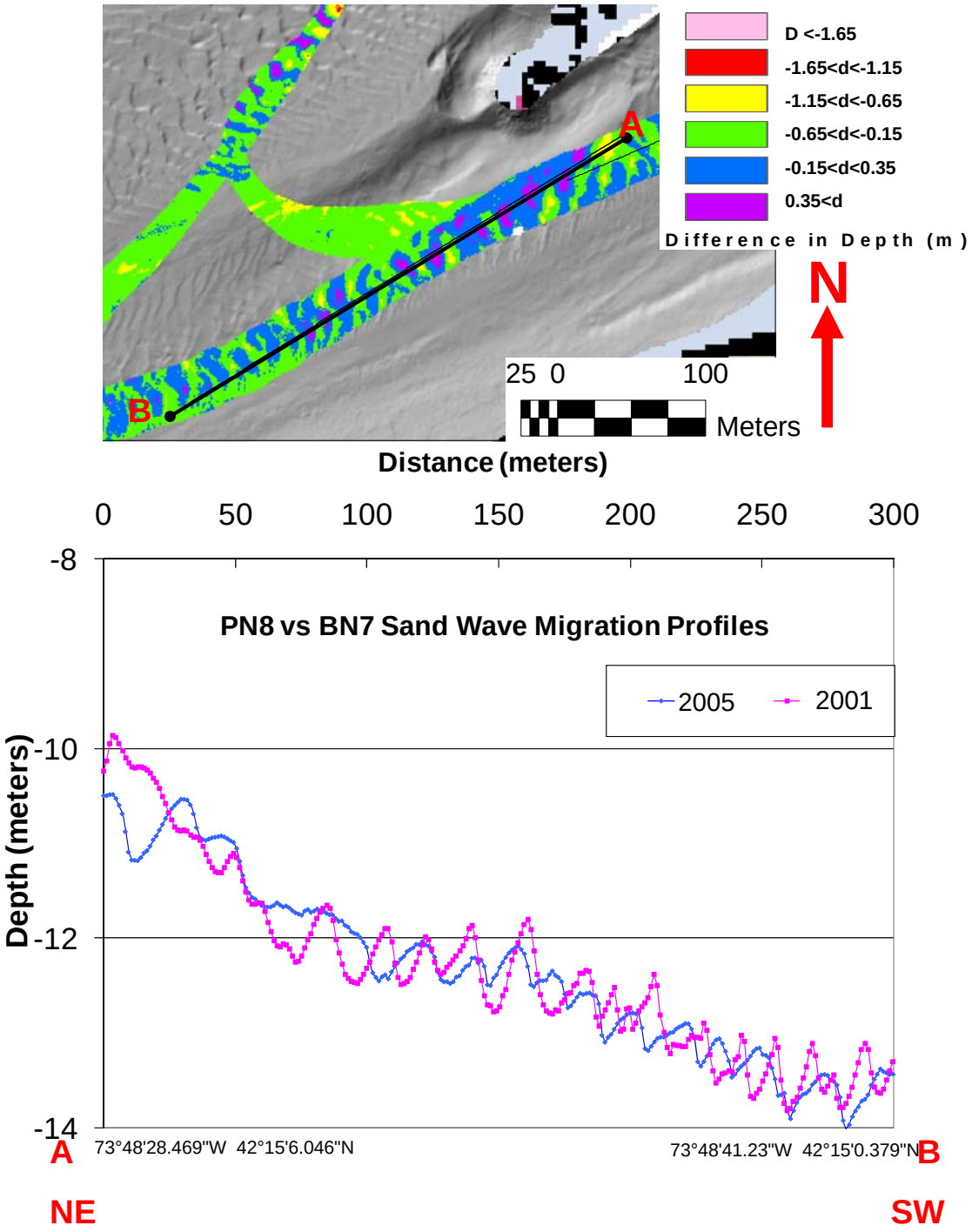
D <-1.65
-1.65<d<-1.15
-1.15<d<-0.65
-0.65<d<-0.15
-0.15<d<0.35
0.35<d
Difference in Depth (m)
A
B
N
25 0 100
Meters
Distance (meters)
0 50 100 150 200 250 300
-8
-10
-12
-14
Depth (meters)
PN8 vs BN7 Sand Wave Migration Profiles
2005
2001
A
73°48'28.469"W 42°15'6.046"N
73°48'41.23"W 42°15'0.379"N
B
NE
SW

Figure 6: The map shows the difference in depth between 2001 and 2005 surveys. This depth difference is plotted on top of the sun illuminated bathymetry of the 2001survey in section PN8.

The graph below shows the depth profile from A-B, the blue line is the depth during the 2005 survey and the pink line is the depth data from the 2001 survey.

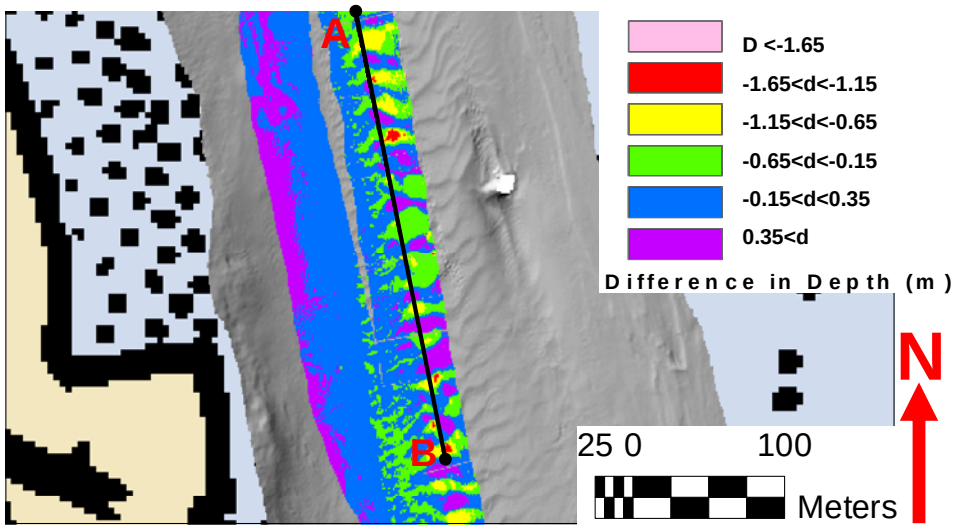
A
B
D <-1.65
-1.65<d<-1.15
-1.15<d<-0.65
-0.65<d<-0.15
-0.15<d<0.35
0.35<d
Difference in Depth (m)
N
25 0 100
Meters

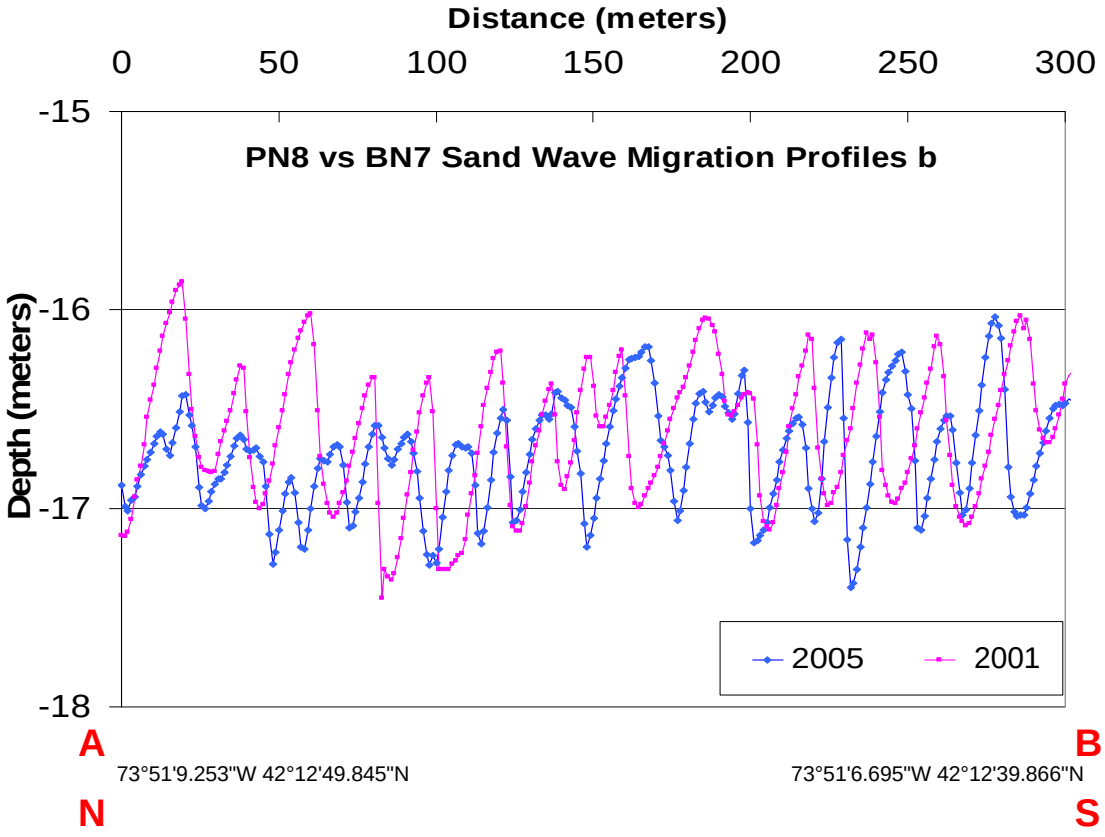
Distance (meters)
0
50
100
150
200
250
300
-15
-16
-17
-18
Depth (meters)
PN8 vs BN7 Sand Wave Migration Profiles b
2005
2001
A
B
73°51'9.253"W 42°12'49.845"N
73°51'6.695"W 42°12'39.866"N
N
S

Figure 7: The map shows the difference in depth between 2001 and 2005 surveys. This depth difference is plotted on top of the sun illuminated bathymetry of the 2001 survey in section PN7.

The graph below shows the depth profile from A-B, the blue line is the depth during the 2005 survey and the pink line is the depth data from the 2001 survey.

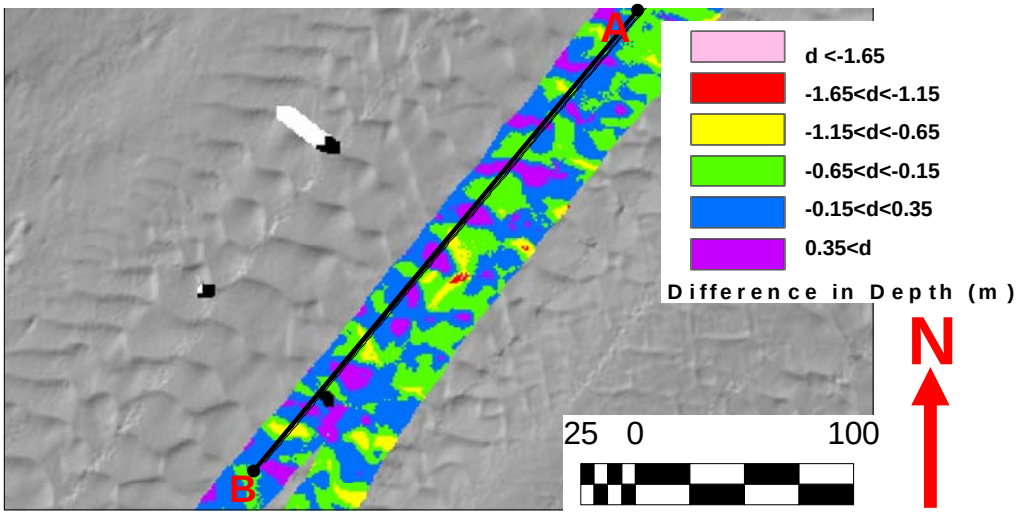
A
B
d <-1.65
-1.65<d<-1.15
-1.15<d<-0.65
-0.65<d<-0.15
-0.15<d<0.35
0.35<d
Difference in Depth (m)
N
25 0 100

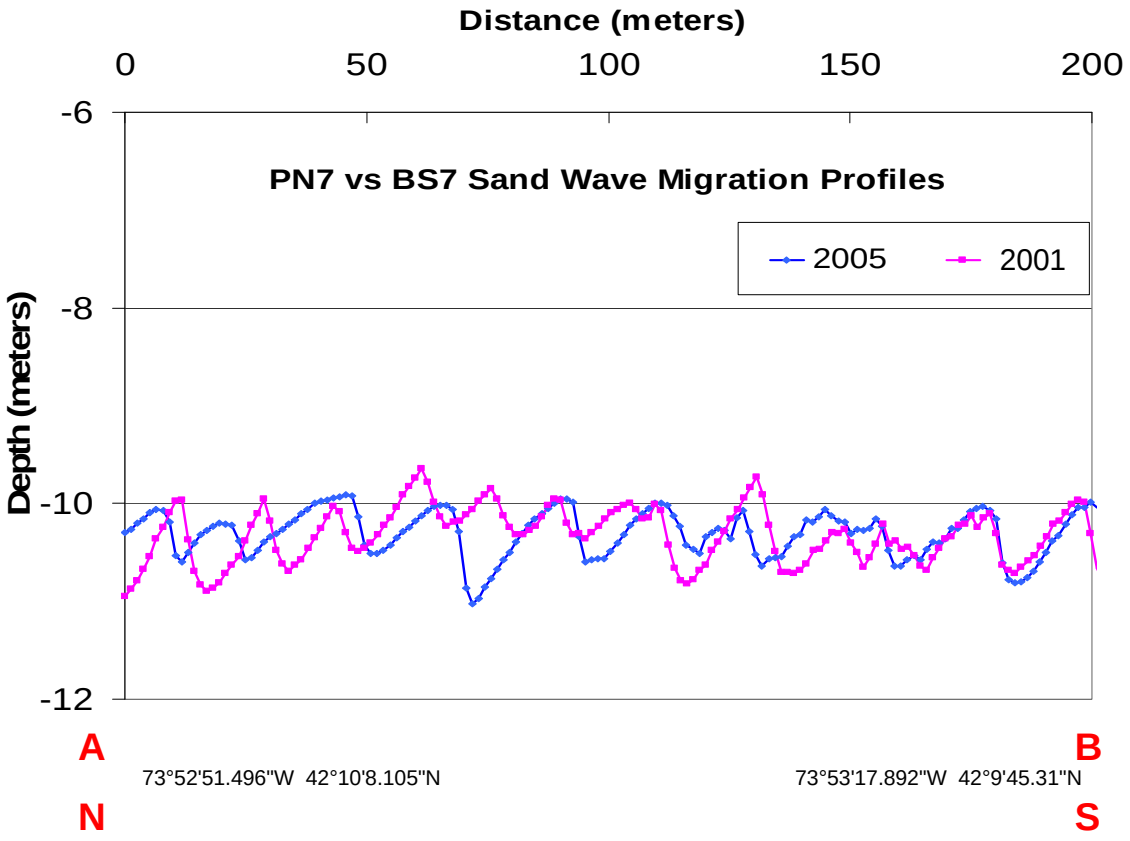
Distance (meters)
0
50
100
150
200
-6
-8
-10
-12
PN7 vs BS7 Sand Wave Migration Profiles
2005
2001
Depth (meters)
A
B
73°52'51.496"W 42°10'8.105"N
73°53'17.892"W 42°9'45.31"N
N
S

Figure 8: The top map shows the difference in depth between 2001 and 2005 surveys. This depth difference is plotted on top of the sun illuminated bathymetry of the 2001 survey in section PN7. The top map is an image of the sun illuminated bathymetry from the 2001 survey.

The graphs on the next page show the depth profile from A-B, the blue line is the depth during the 2005 survey and the pink line is the depth data from the 2001 survey.

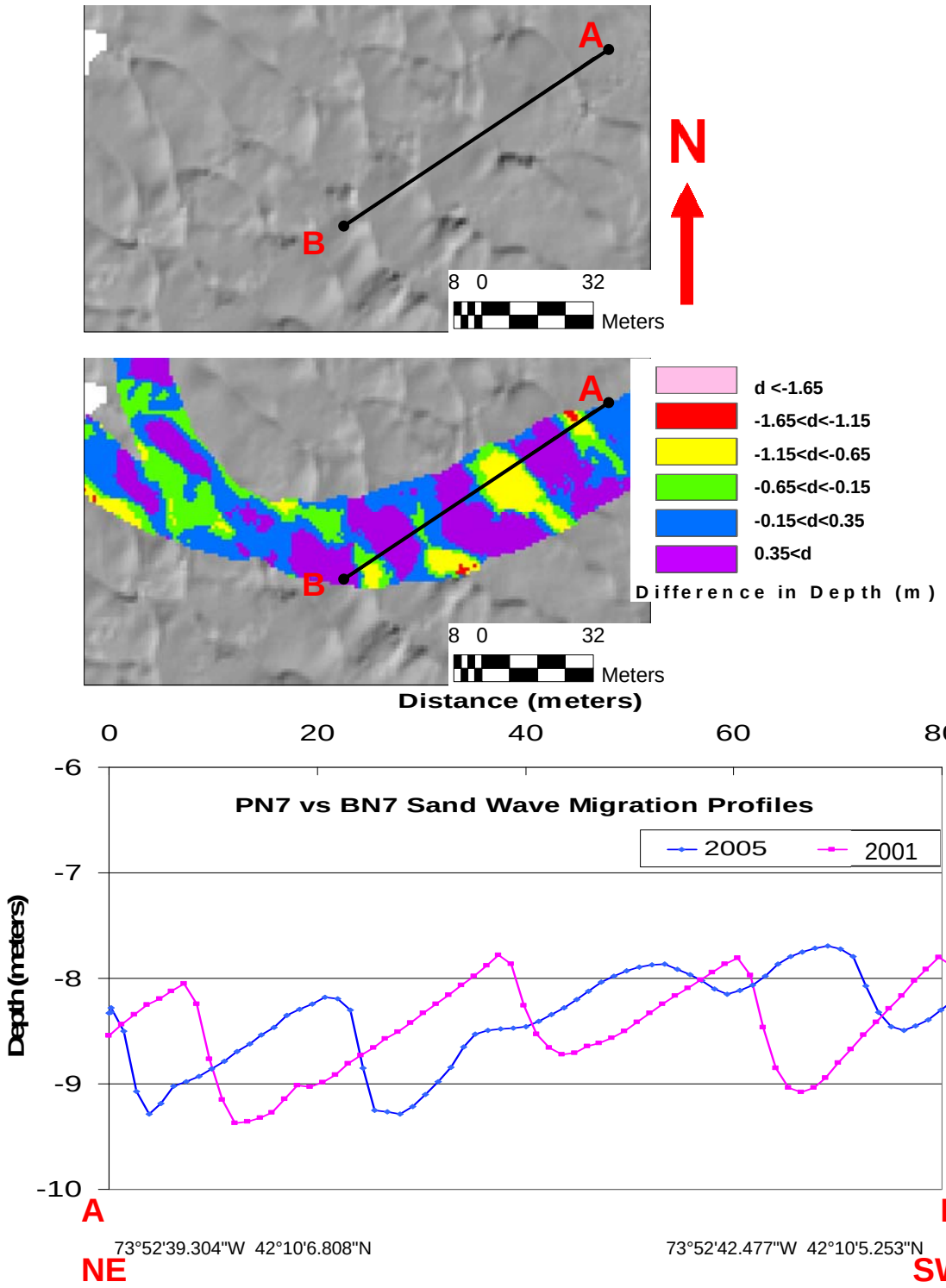
A
B
N
8 0 32
Meters
d <-1.65
-1.65<d<-1.15
-1.15<d<-0.65
-0.65<d<-0.15
-0.15<d<0.35
0.35<d
Difference in Depth (m)
Distance (meters)
0
20
40
60
80
PN7 vs BN7 Sand Wave Migration Profiles
2005
2001
Depth (meters)
-6
-7
-8
-9
-10
73°52'39.304"W 42°10'6.808"N
73°52'42.477"W 42°10'5.253"N
NE
SW

Figure 9: The map on the bottom left shows the difference in depth between 1998 and 2005 surveys. This depth difference is plotted on top of the 1998 sun illuminated bathymetry. The map on the top left is a plot of 1998 sun illuminated bathymetry (light grey), and the map on the top right is the 2005 sun illuminated bathymetry plotted on top of the 1998 sun illuminated bathymetry. These maps images are from section PN6.

The graph below shows the depth profile from A-B, the blue line is the depth during the 2005 survey and the pink line is the depth data from the 1998 survey.

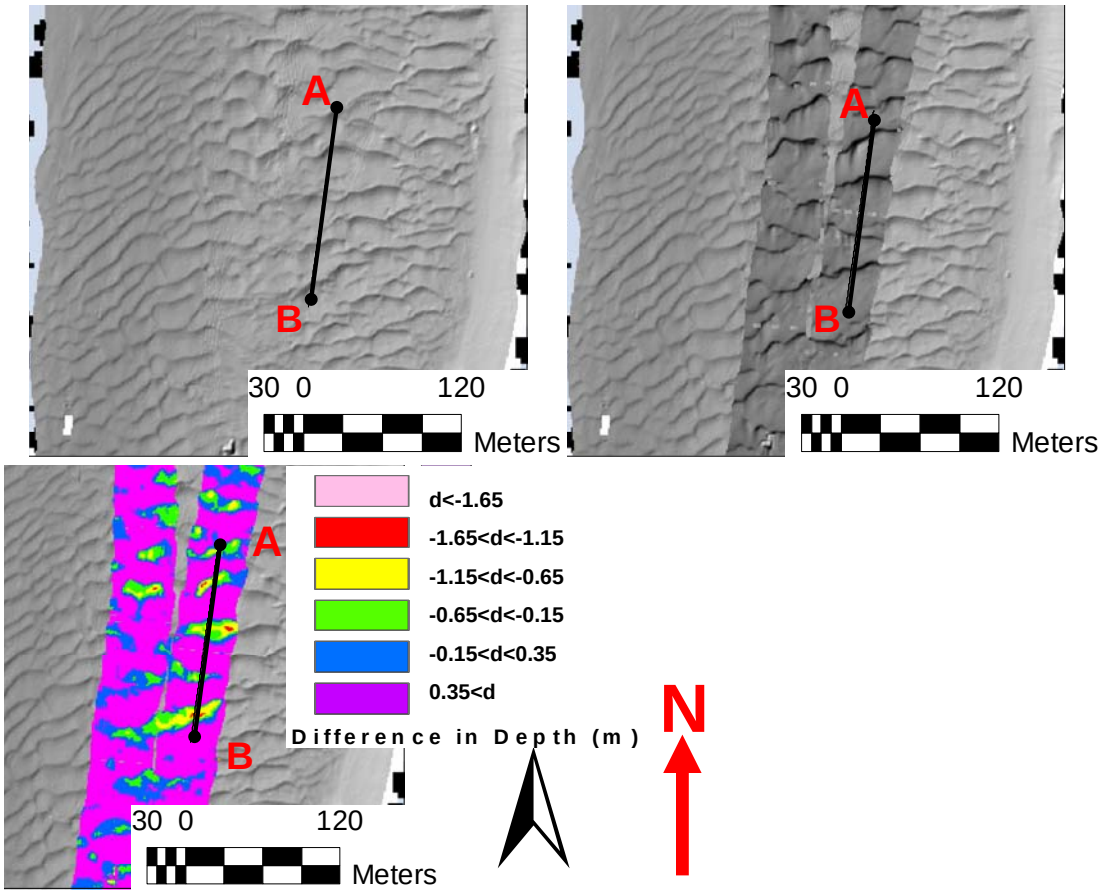
A
B
30 0 120
Meters
A
B
30 0 120
Meters
A
B
30 0 120
Meters
d<-1.65
-1.65<d<-1.15
-1.15<d<-0.65
-0.65<d<-0.15
-0.15<d<0.35
0.35<d
Difference in Depth (m)
N

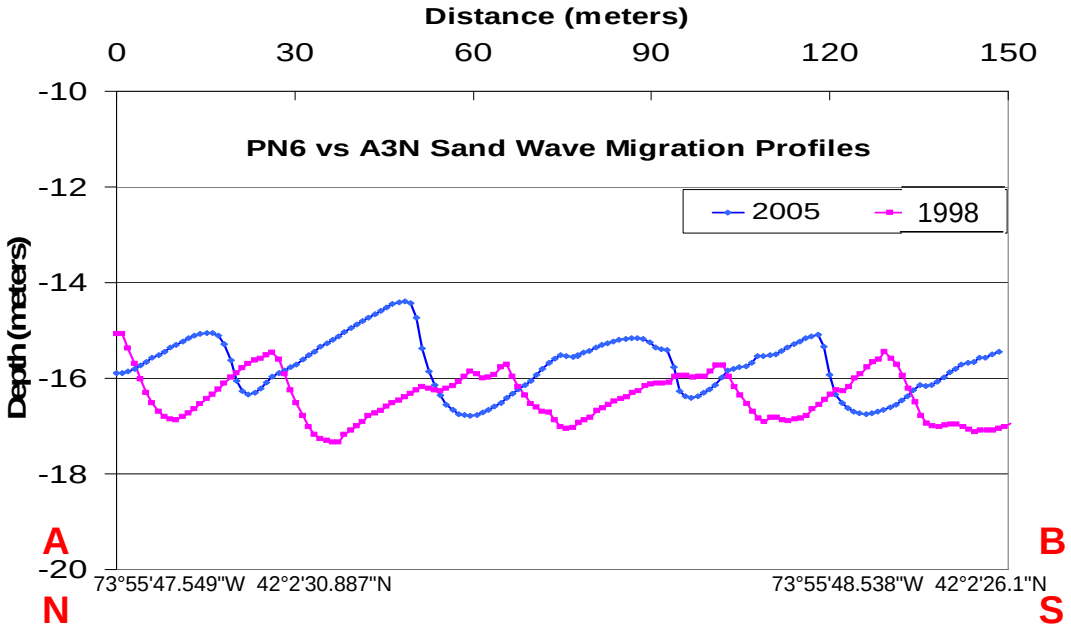
Distance (meters)
0
30
60
90
120
150
-10
-12
-14
-16
-18
-20
Depth (meters)
PN6 vs A3N Sand Wave Migration Profiles
2005
1998
A
B
73°55'47.549"W 42°2'30.887"N
73°55'48.538"W 42°2'26.1"N
N
S

Figure 10: The map on the bottom left shows the difference in depth between 1998 and 2005 surveys. This depth difference is plotted on top of the sun illuminated bathymetry of the 1998. The map on the top left is a plot of 1998 sun illuminated bathymetry (light grey), and the map on the top right is the 2005 sun illuminated bathymetry plotted on top of the 1998 sun illuminated bathymetry. These maps images are from section PN4.

The graph below shows the depth profile from A-B, the blue line is the depth during the 2005 survey and the pink line is the depth data from the 1998 survey.

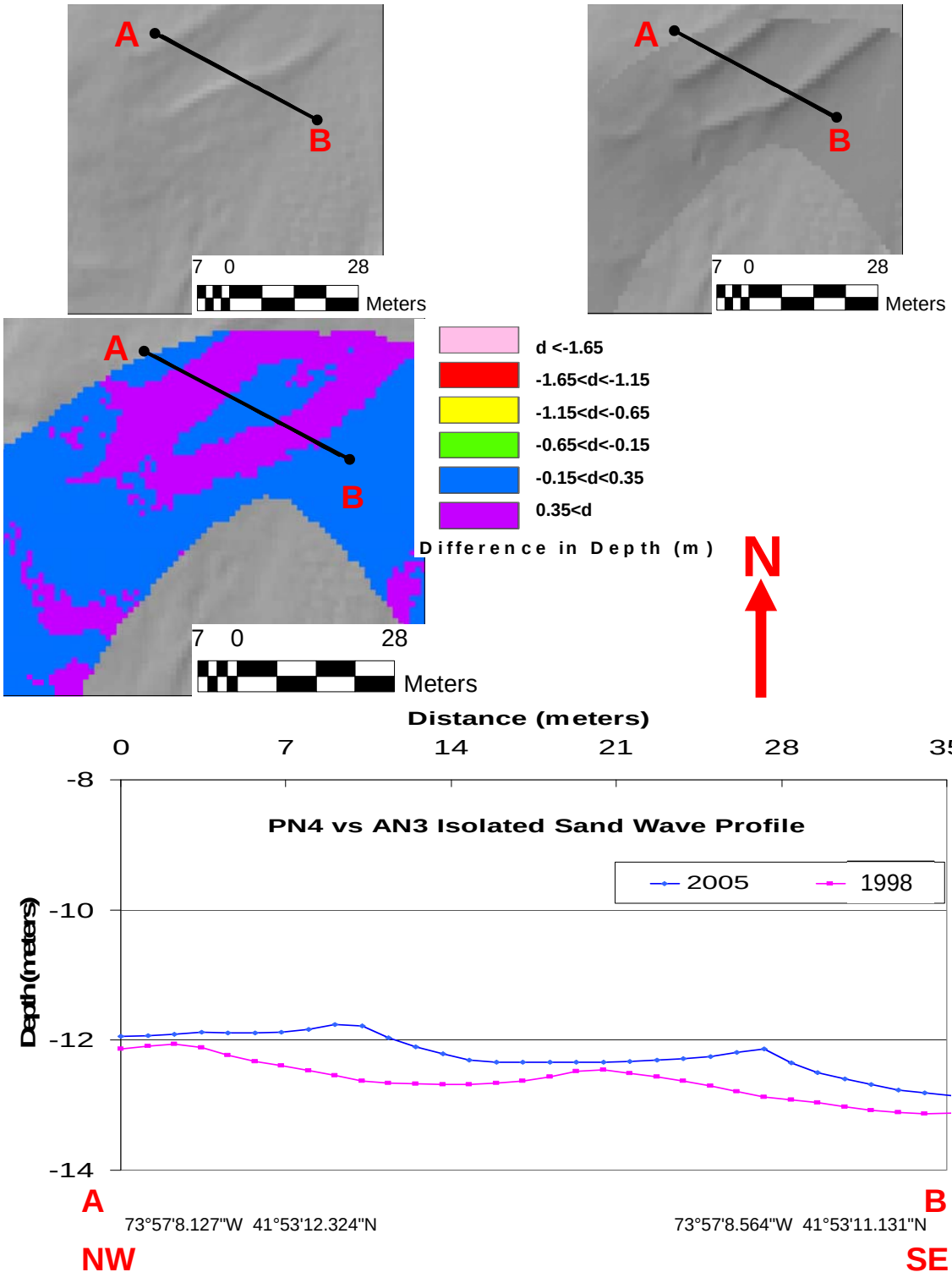
A
B
7 0 28
Meters
A
B
7 0 28
Meters
A
B
7 0 28
Meters
d <-1.65
-1.65<d<-1.15
-1.15<d<-0.65
-0.65<d<-0.15
-0.15<d<0.35
0.35<d
Difference in Depth (m)
N
Distance (meters)
0 7 14 21 28 35
-8
-10
-12
-14
PN4 vs AN3 Isolated Sand Wave Profile
2005
1998
Depth(meters)
A
B
73°57'8.127"W 41°53'12.324"N
73°57'8.564"W 41°53'11.131"N
NW
SE

Figure 11 (Top): The map on the top left is the sun illuminated bathymetry from the 1998-2003 (light grey) survey. The map on the bottom shows the sun illuminated bathymetry from the 2005 survey (dark grey) on top of the 2003 sun illuminated bathymetry from 2003 (light grey). These maps are from section WS6.

Figure 12 (Bottom): The map on the bottom left the sun illuminated bathymetry from the 1998-2003 (light grey) survey. The map on the bottom right shows the sun illuminated bathymetry from the 2005 survey (dark grey) on top of the 2003 sun illuminated bathymetry from 2003 (light grey). These maps are from section WS6.

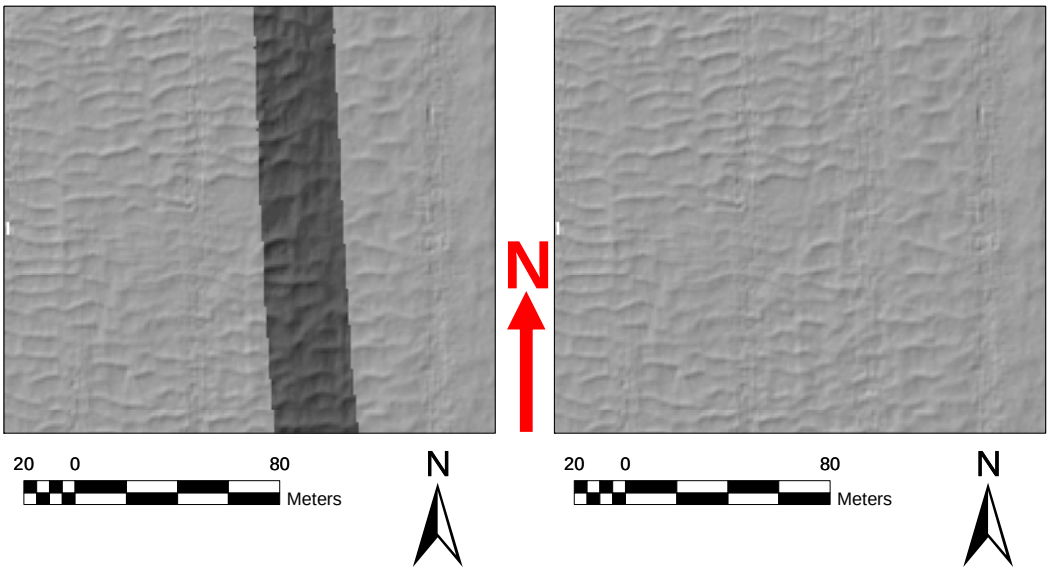
20 0 80
Meters
N
N
20 0 80
Meters
N

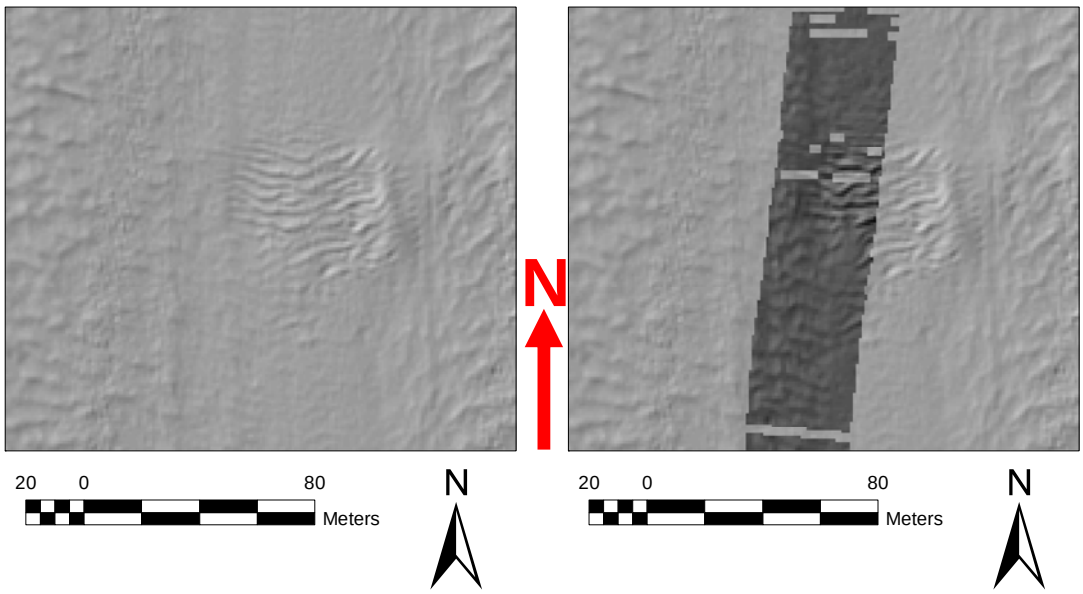
20 0 80
Meters
N
N
20 0 80
Meters
N

Figure 13: The map on the left shows the sun illuminated bathymetry from the 2003 survey. The map on the right shows the sun illuminated bathymetry from the 2005 survey (dark grey) on top of the 2003 sun illuminated bathymetry from 2003 (light grey). These maps are from section WS7.

The graph below shows the depth profile from A-B, the blue line is the depth during the 2005 survey and the pink line is the depth data from the 2003 survey.

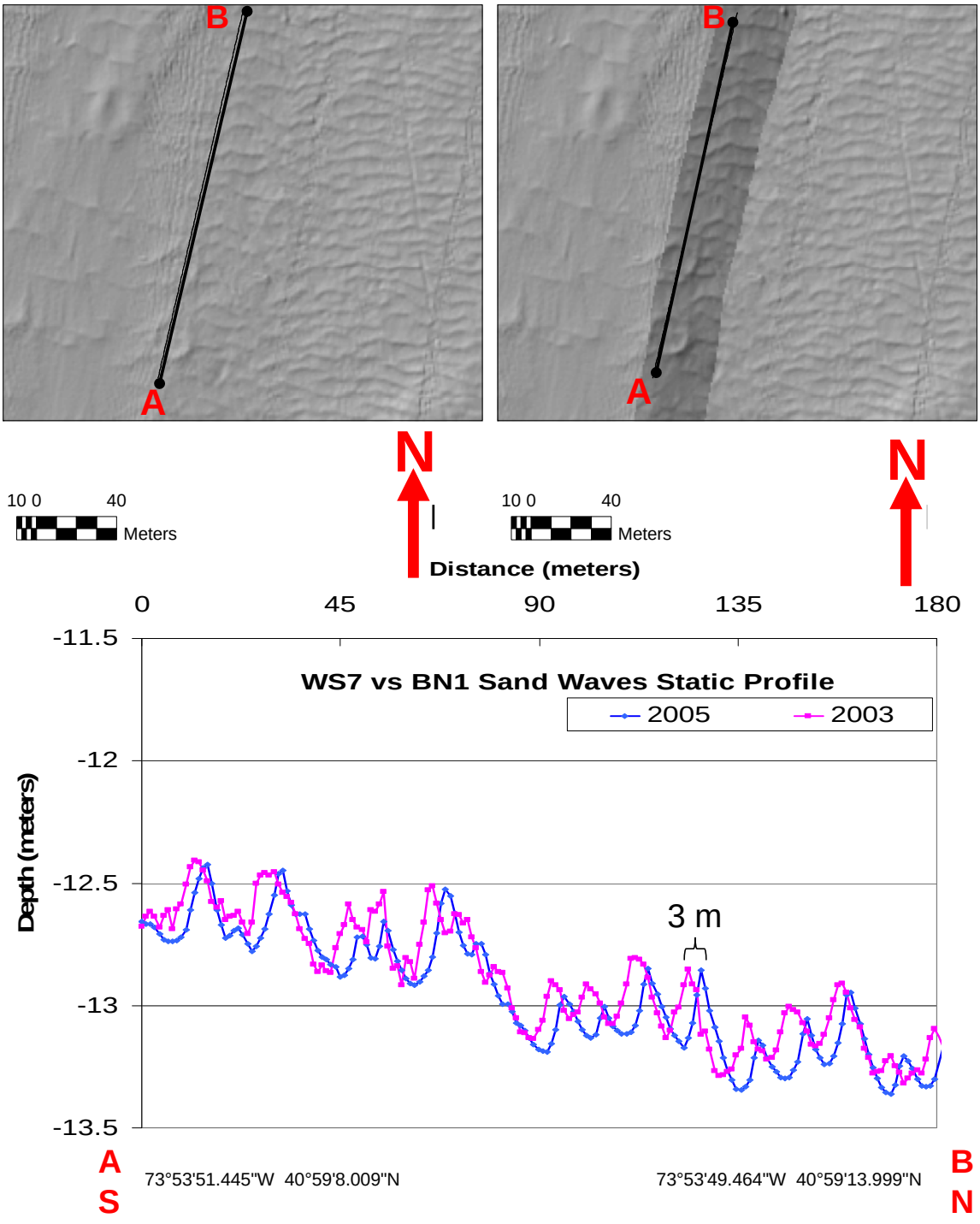
B
A
B
A
N
10 0 40
Meters
N
10 0 40
Meters
Distance (meters)
0 45 90 135 180
WS7 vs BN1 Sand Waves Static Profile
2005
2003
Depth (meters)
-11.5
-12
-12.5
-13
-13.5
3 m
A
S
73°53'51.445"W 40°59'8.009"N
73°53'49.464"W 40°59'13.999"N
B
N

Figure 14: The map below show the difference in depth between 2001 and 2005 surveys. This depth difference is plotted on top of the sun illuminated bathymetry of the 2001 survey in section PN8.

The graph below shows the depth profile from A-B, the blue line is the depth during the 2005 survey and the pink line is the depth data from the 2001 survey.

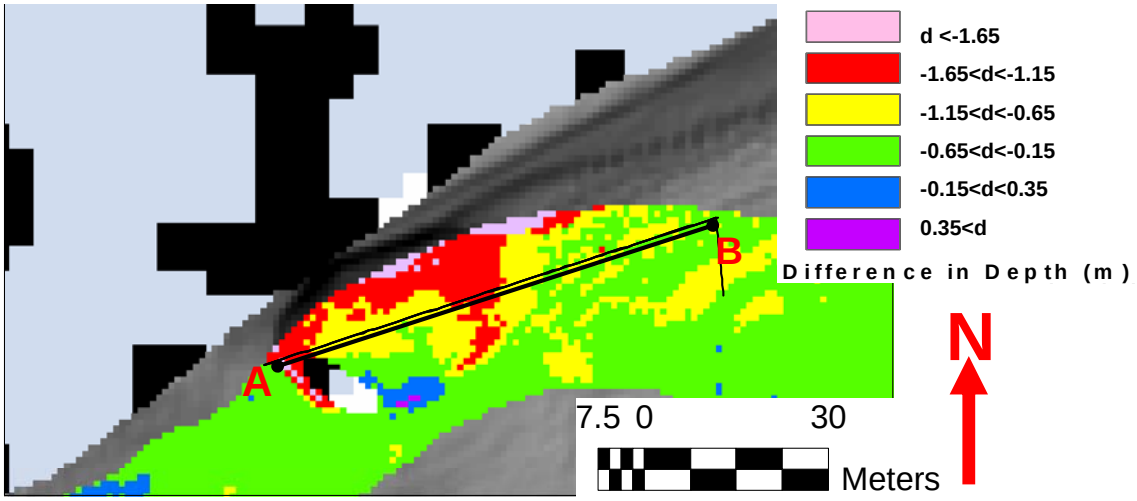
d <-1.65
-1.65<d<-1.15
-1.15<d<-0.65
-0.65<d<-0.15
-0.15<d<0.35
0.35<d
Difference in Depth (m)
A
B
7.5 0
30
Meters
N

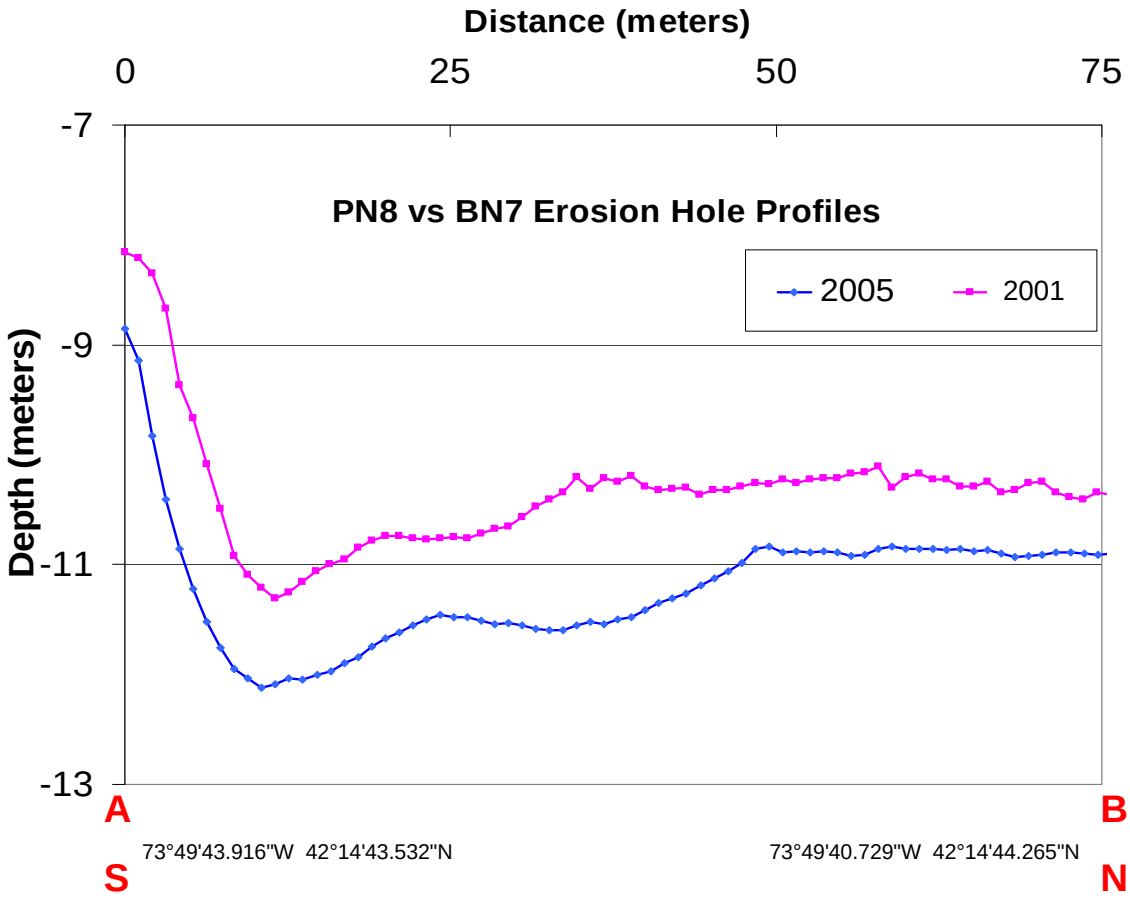
Distance (meters)
0
25
50
75
-7
-9
-11
-13
Depth (meters)
PN8 vs BN7 Erosion Hole Profiles
2005
2001
A
B
73°49'43.916"W 42°14'43.532"N
73°49'40.729"W 42°14'44.265"N
S
N

Figure 15: The map shows the sun illuminated bathymetry from the 1999 survey. The black lines are 2 m contours of the 1999 survey data. These images were collected from region PN6.

The graph shows the depth profile from A-B, the blue line is the depth during the 2005 survey and the pink line is the depth data from the 1999 survey.

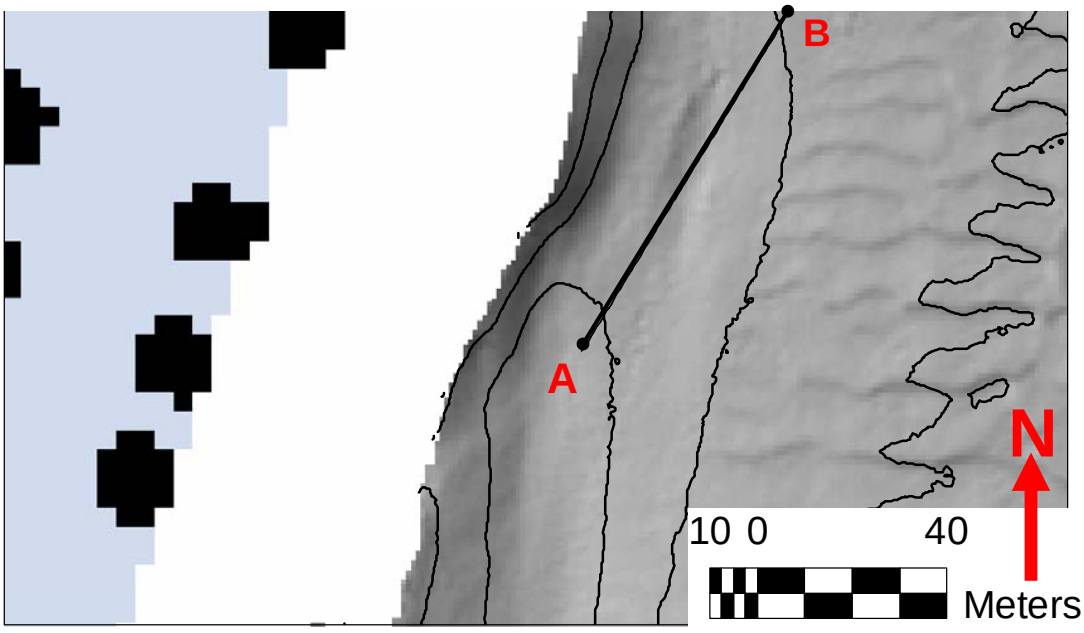
B
A
N
10 0
40
Meters

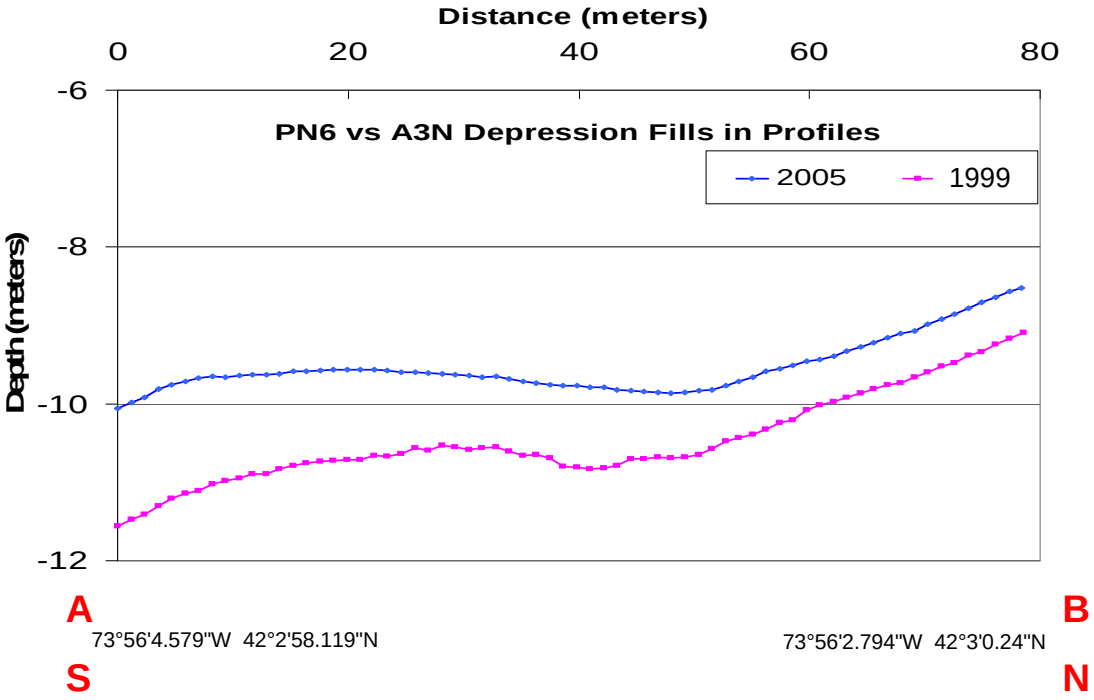
Distance (meters)
0
20
40
60
80
-6
-8
-10
-12
Depth (meters)
PN6 vs A3N Depression Fills in Profiles
2005
1999
A
S
73°56'4.579"W 42°2'58.119"N
B
N
73°56'2.794"W 42°3'0.24"N

Figure 16: The map below shows the sun illuminated bathymetry from the 2003 survey. The black lines are 2 m contours of the 2003 and 2005 survey data. These images were collected from region PN4.

The graph below shows the depth profile from A-B, the blue line is the depth during the 2005 survey and the pink line is the depth data from the 2003 survey.

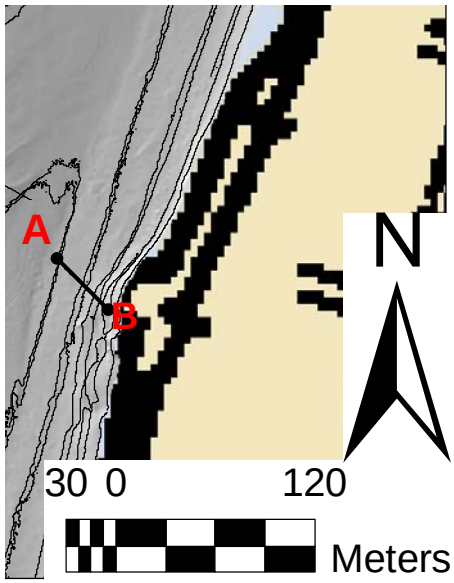
A
B
N
30 0
120
Meters

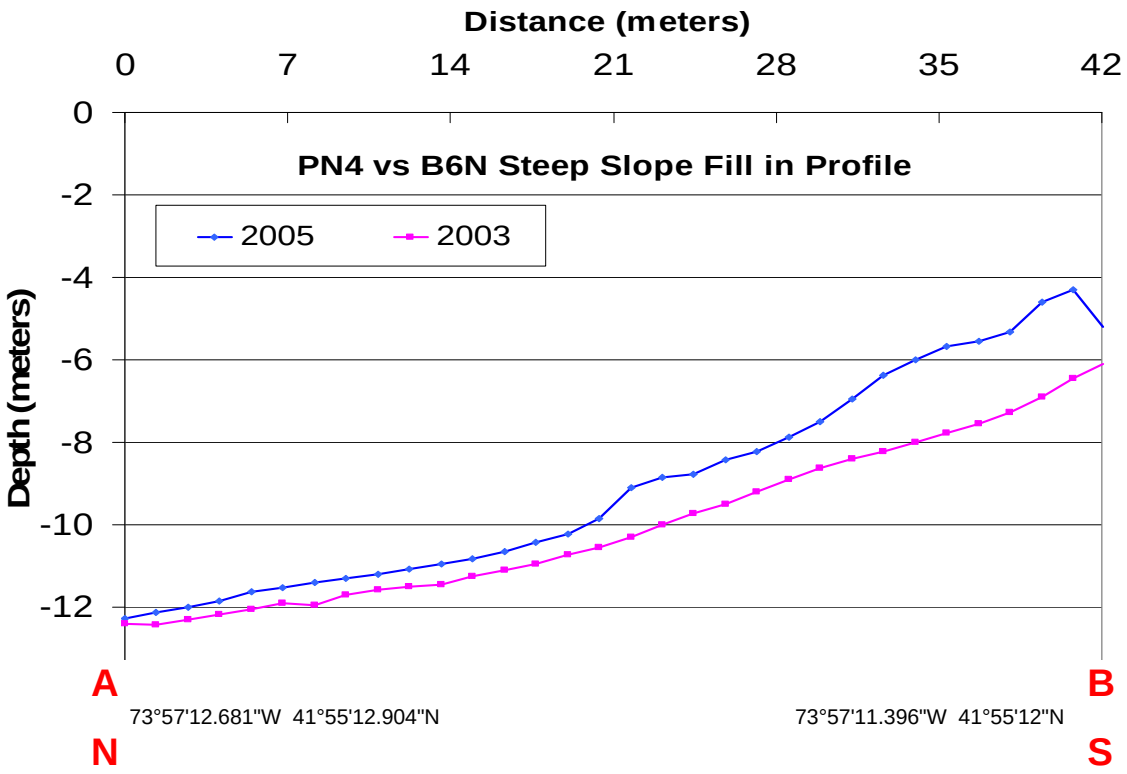
Distance (meters)
0
7
14
21
28
35
42
PN4 vs B6N Steep Slope Fill in Profile
2005
2003
Depth (meters)
0
-2
-4
-6
-8
-10
-12
A
B
73°57'12.681"W 41°55'12.904"N
73°57'11.396"W 41°55'12"N
N
S

Figure 17: The map on the bottom left shows the difference in depth between 2001 and 2005 surveys. This depth difference is plotted on top of the sun illuminated bathymetry of the 2001 survey in section PN8. The map on the top right is a plot of 2001 sun illuminated bathymetry, and the map on the top right is the 2005 sun illuminated bathymetry.

The graph below shows the depth profile from A-B, the blue line is the depth during the 2005 survey and the pink line is the depth data from the 2001 survey.

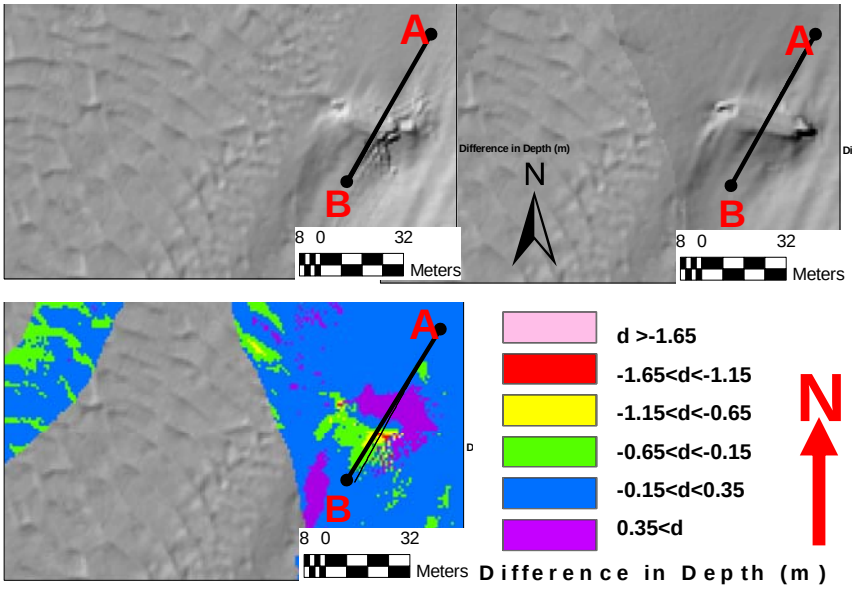
A
B
8 0 32
Meters
Difference in Depth (m)
N
d >-1.65
-1.65<d<-1.15
-1.15<d<-0.65
-0.65<d<-0.15
-0.15<d<0.35
0.35<d
Difference in Depth (m)

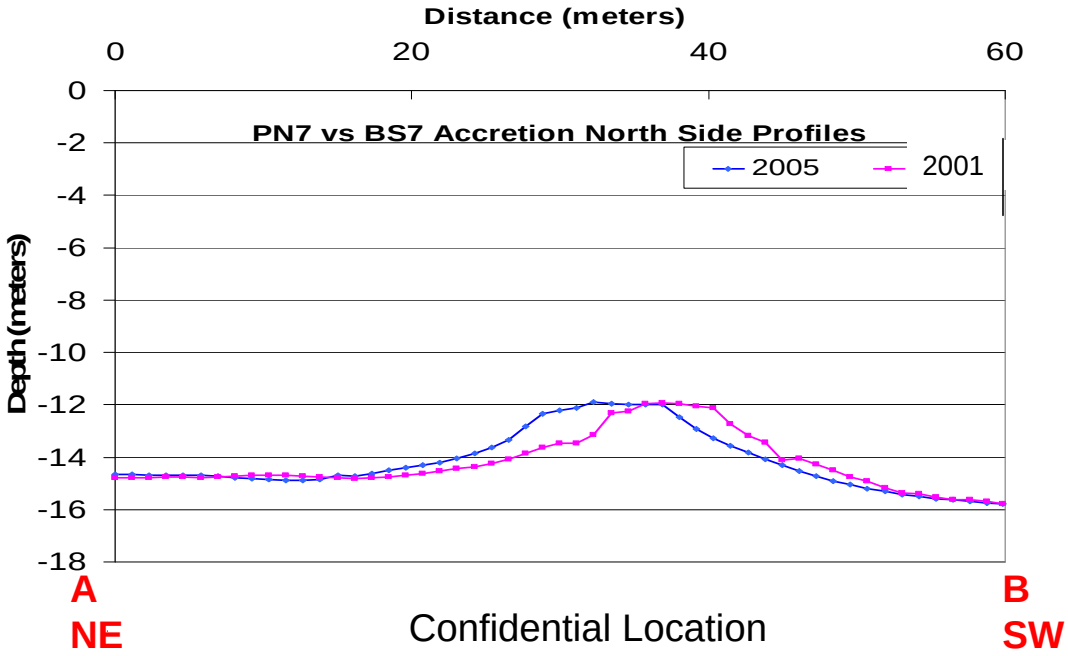
Distance (meters)
0
20
40
60
PN7 vs BS7 Accretion North Side Profiles
2005
2001
Depth (meters)
0
-2
-4
-6
-8
-10
-12
-14
-16
-18
A
NE
Confidential Location
B
SW

Figure 18: The map on the top shows the sun illuminated bathymetry from the 2001 survey. The map on the bottom shows the sun illuminated bathymetry from the 2005 survey (dark grey) on top of the 2001 sun illuminated bathymetry from 2001 (light grey). These maps are from section PN6

The graph below shows the depth profile from A-B, the blue line is the depth during the 2005 survey and the pink line is the depth data from the 2001 survey. The lines protruding vertically from the profiles are depth error bars representing 1 m difference.

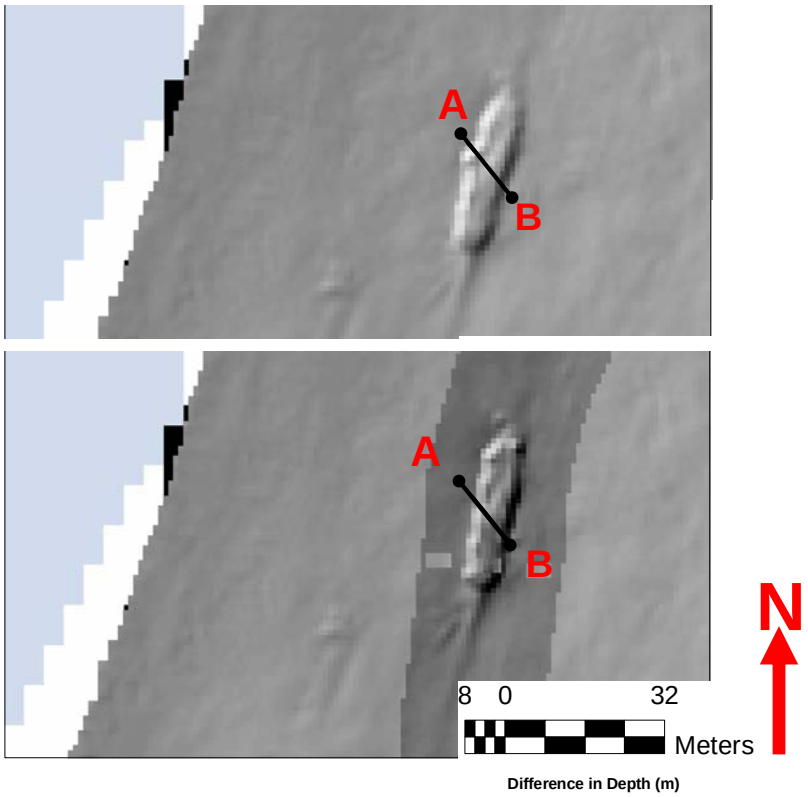
A
B
A
B
N
8 0 32
Meters
Difference in Depth (m)

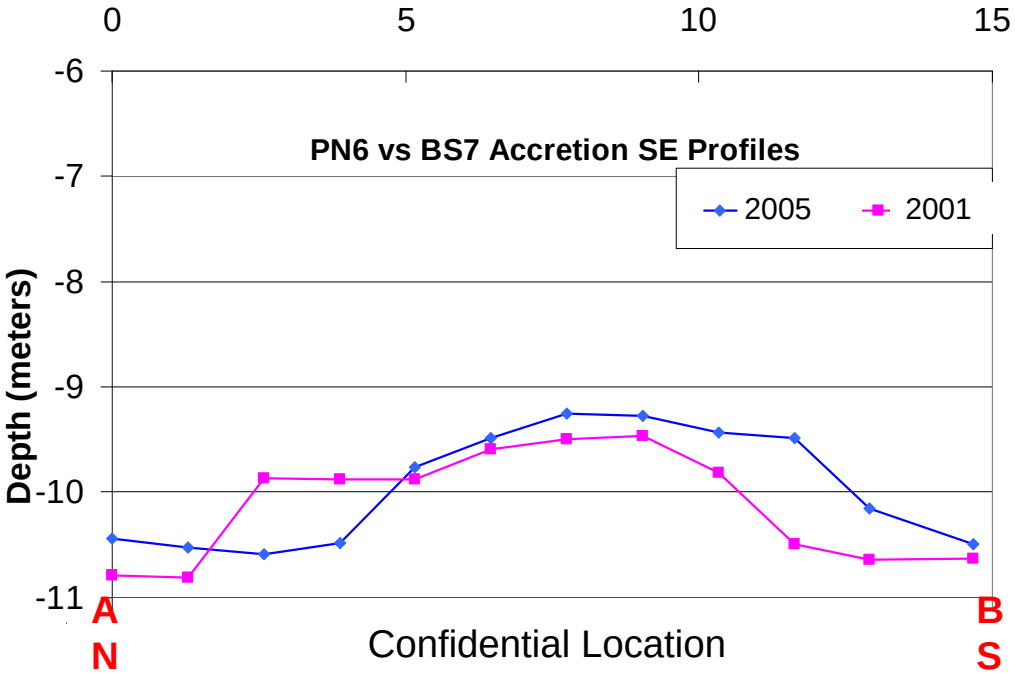
Distance (meters)
0
5
10
15
-6
-7
-8
-9
-10
-11
Depth (meters)
PN6 vs BS7 Accretion SE Profiles
2005
2001
A
N
B
S
Confidential Location

Figure 19: The map below show the difference in depth between 2003 and 2005 surveys. This depth difference is plotted on top of the sun illuminated bathymetry of the 2003 survey in section PN3.

The graph below shows the depth profile from A-B, the blue line is the depth during the 2005 survey and the pink line is the depth data from the 2003 survey.

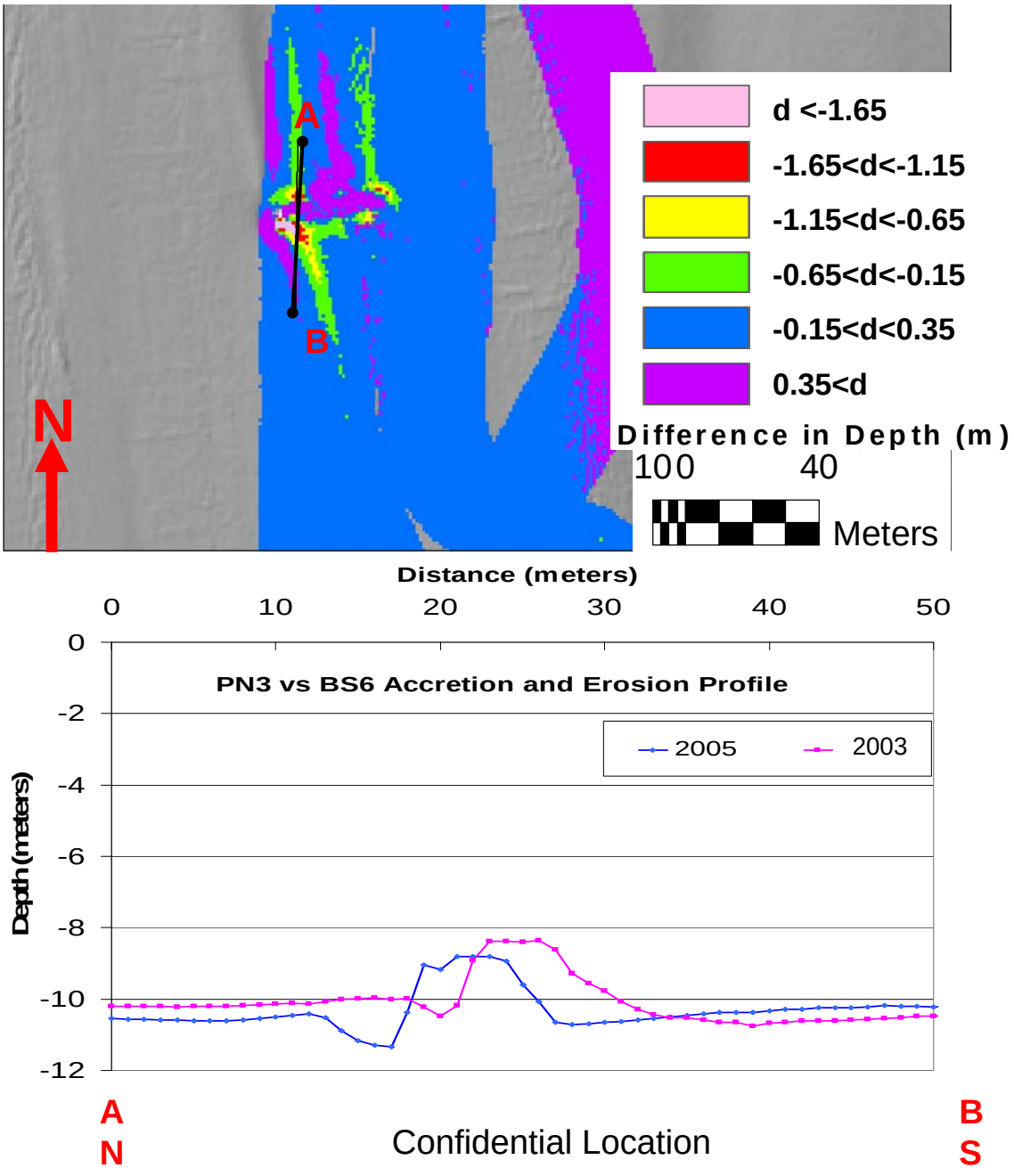
A
B
N
d <-1.65
-1.65<d<-1.15
-1.15<d<-0.65
-0.65<d<-0.15
-0.15<d<0.35
0.35<d
Difference in Depth (m)
100
40
Meters
Distance (meters)
0
10
20
30
40
50
PN3 vs BS6 Accretion and Erosion Profile
2005
2003
Depth (meters)
0
-2
-4
-6
-8
-10
-12
A
N
Confidential Location
B
S

Figure 20: The map below shows the difference in depth between 2003 and 2005 surveys. This depth difference is plotted on top of the sun illuminated bathymetry of the 2003 survey in section PN1.

The graph below shows the depth profile from A-B, the blue line is the depth during the 2005 survey and the pink line is the depth data from the 2003 survey.

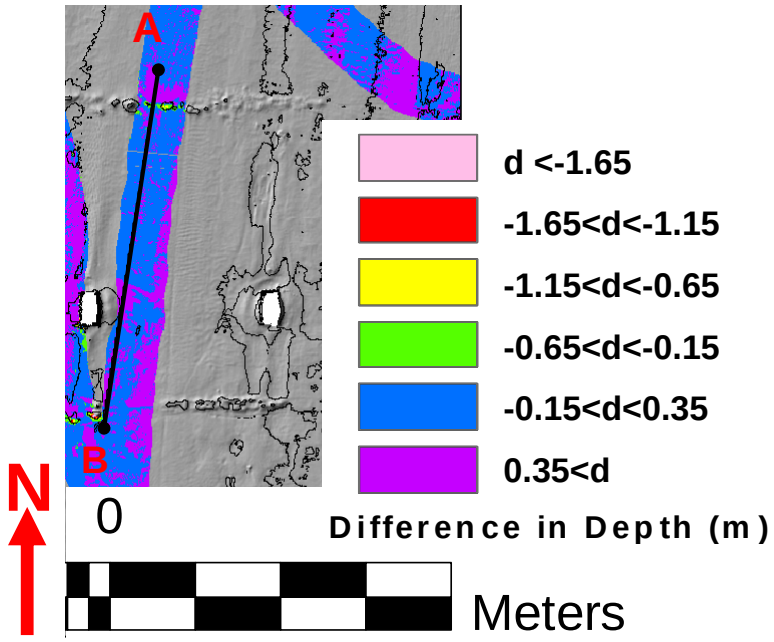
A
B
N
0
d <-1.65
-1.65<d<-1.15
-1.15<d<-0.65
-0.65<d<-0.15
-0.15<d<0.35
0.35<d
Difference in Depth (m)
Meters

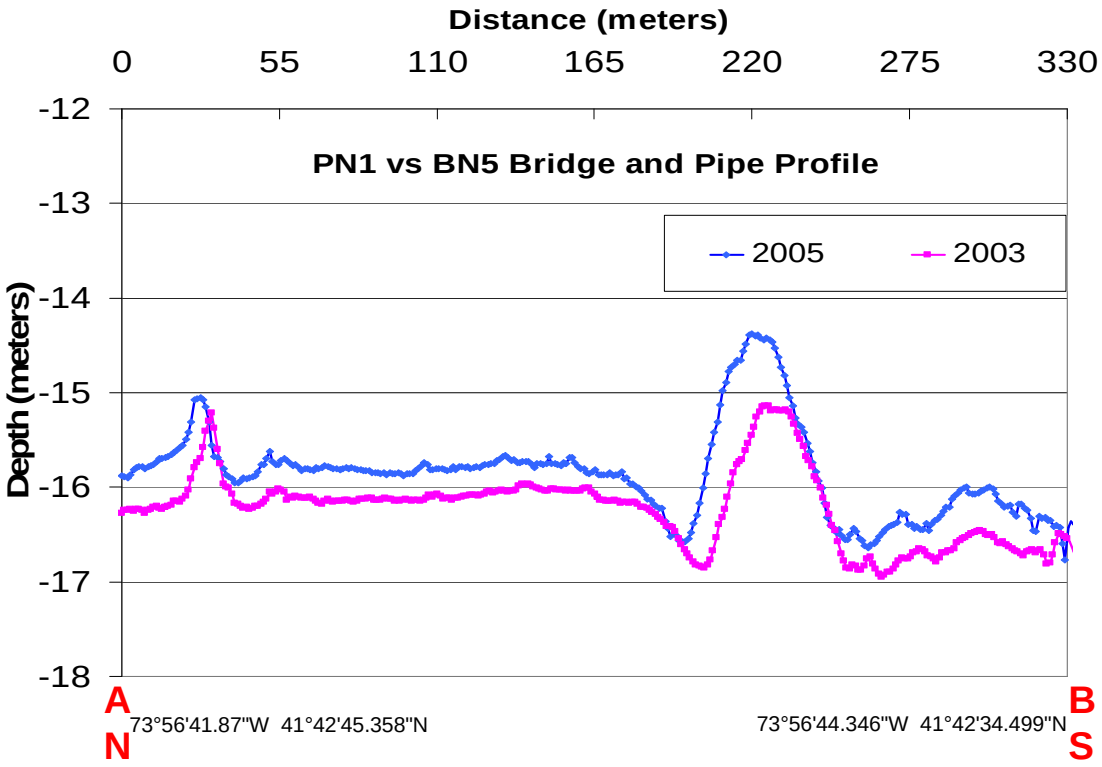
Distance (meters)
0
55
110
165
220
275
330
-12
-13
-14
-15
-16
-17
-18
PN1 vs BN5 Bridge and Pipe Profile
2005
2003
Depth (meters)
A
N
73°56'41.87"W 41°42'45.358"N
73°56'44.346"W 41°42'34.499"N
B
S

Figure 21: The map on the top shows the sun illuminated bathymetry from the 2003 survey. The map on the bottom shows the sun illuminated bathymetry from the 2005 survey (dark grey) on top of the 2003 sun illuminated bathymetry from 2003 (light grey). These maps are from section WO.

The graph below shows the depth profile from A-B, the blue line is the depth during the 2005 survey and the pink line is the depth data from the 2003 survey.

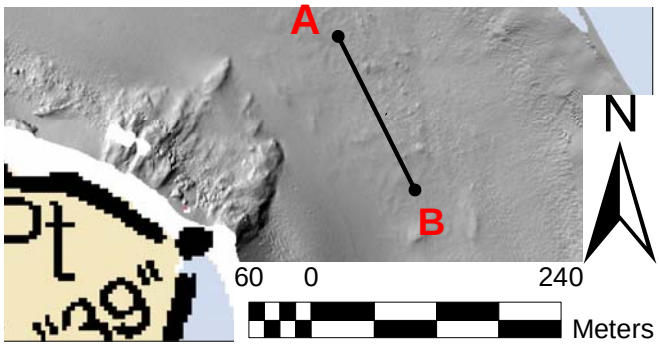
A
B
N
60 0 240
Meters

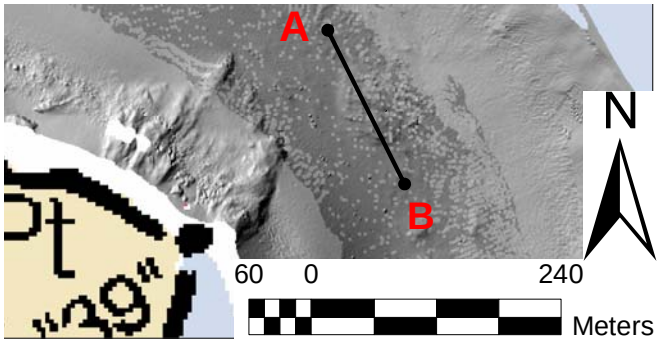
A
B
N
60 0 240
Meters

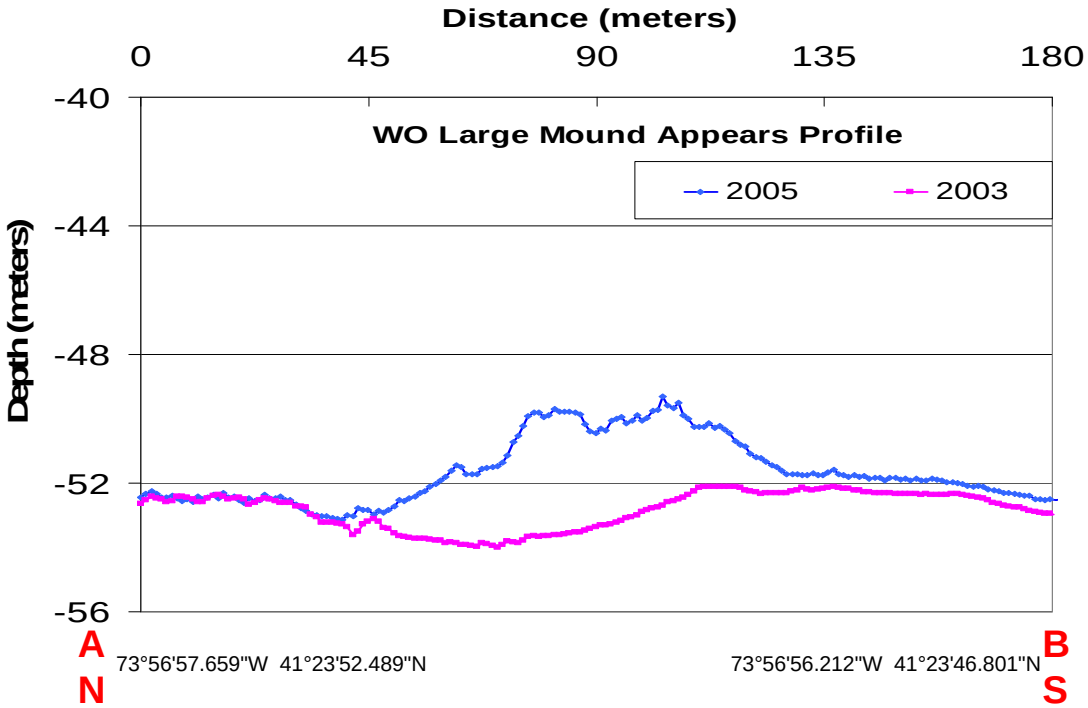
Distance (meters)
0
45
90
135
180
-40
-44
-48
-52
-56
Depth (meters)
WO Large Mound Appears Profile
2005
2003
A
N
73°56'57.659"W 41°23'52.489"N
73°56'56.212"W 41°23'46.801"N
B
S

Figure 22: The map on the left shows the sun illuminated bathymetry from the 2003 survey. The map on the right shows the sun illuminated bathymetry from the 2005 survey (dark grey) on top of the 2003 sun illuminated bathymetry from 2003 (light grey). These maps are from section WS7.

The graph below shows the depth profile from A-B, the blue line is the depth during the 2005 survey and the pink line is the depth data from the 2003 survey.

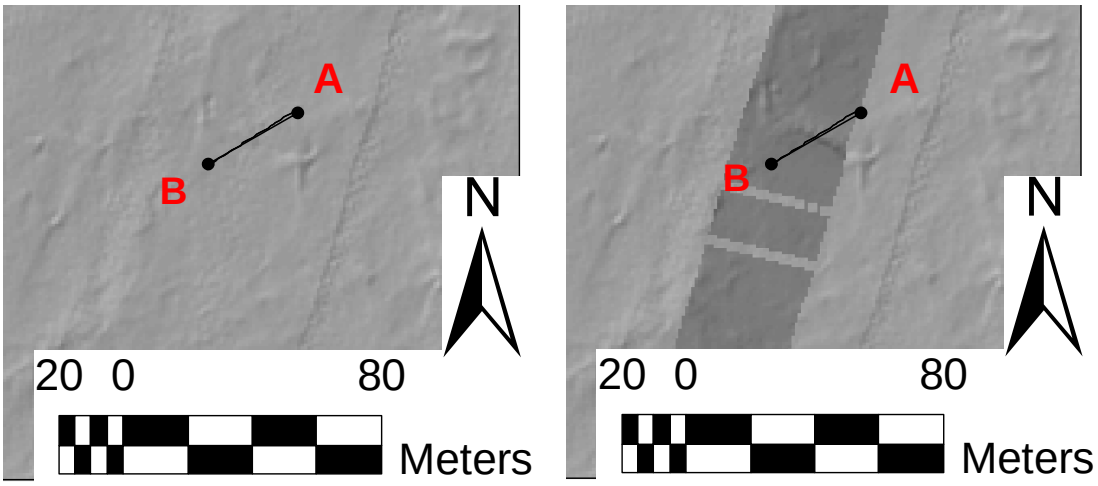
A
B
N
20 0 80
Meters
A
B
N
20 0 80
Meters

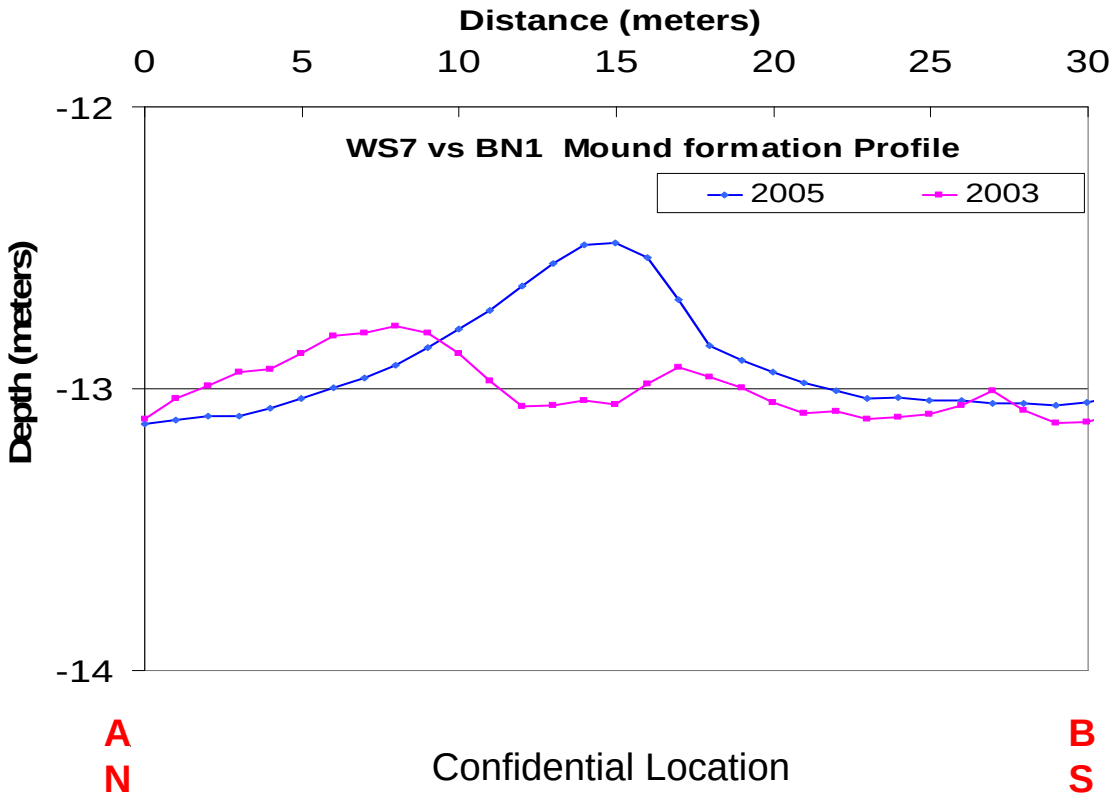
Distance (meters)
0 5 10 15 20 25 30
-12
-13
-14
Depth (meters)
WS7 vs BN1 Mound formation Profile
2005
2003
A
N
Confidential Location
B
S

Figure 23: The map on the top shows the sun illuminated bathymetry from the 2003 survey. The map on the bottom shows the sun illuminated bathymetry from the 2005 survey (dark grey) on top of the 2003 sun illuminated bathymetry from 2003 (light grey). These maps are from section PN2.

The graph below shows the depth profile from A-B, the blue line is the depth during the 2005 survey and the pink line is the depth data from the 2003 survey.

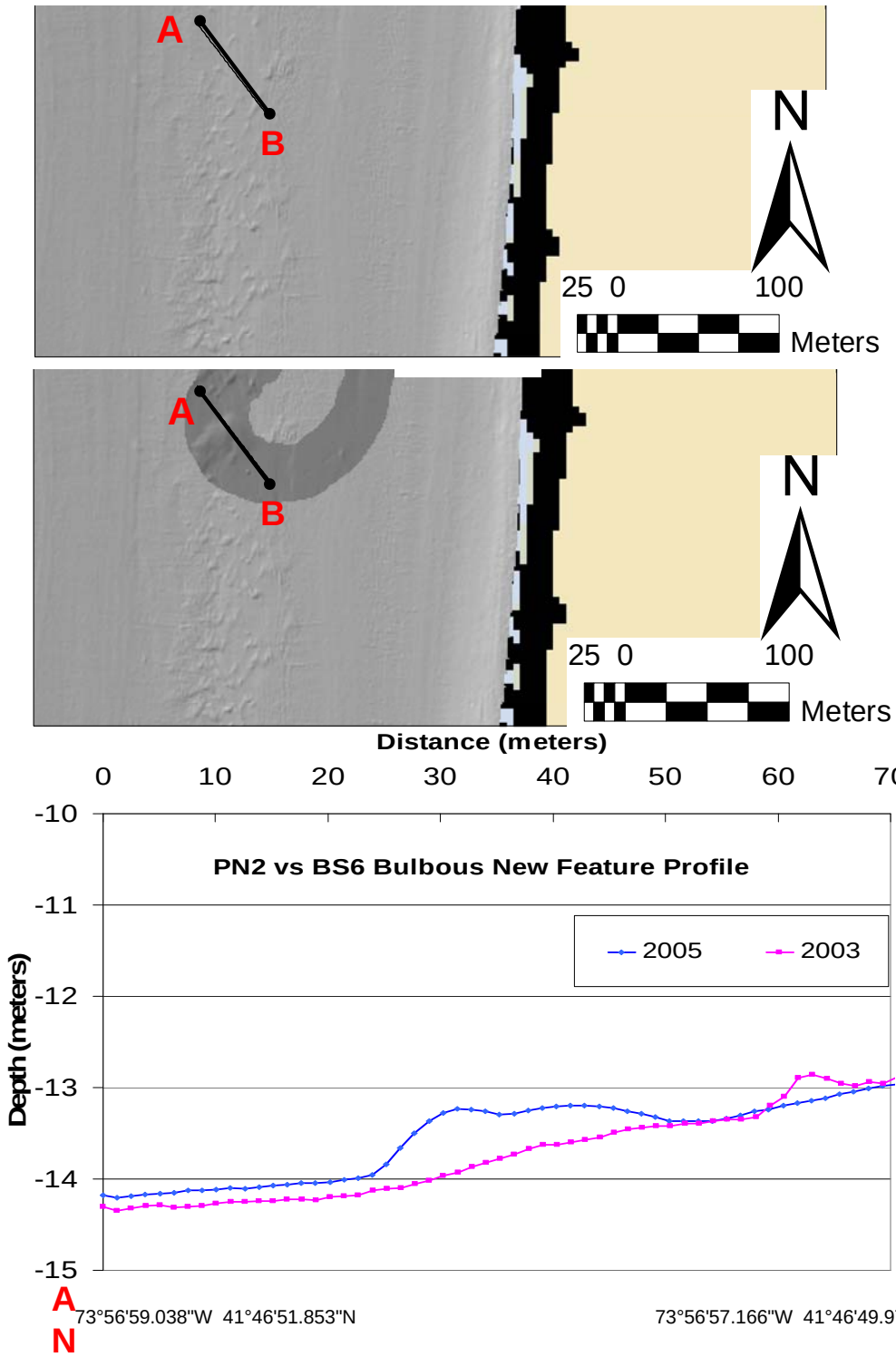
A
B
N
25 0 100
Meters
A
B
N
25 0 100
Meters
Distance (meters)
0 10 20 30 40 50 60 70
PN2 vs BS6 Bulbous New Feature Profile
2005
2003
Depth (meters)
-10
-11
-12
-13
-14
-15
A
N
73°56'59.038"W 41°46'51.853"N
73°56'57.166"W 41°46'49.976"N
B
S

Figure 24: The map on the below shows the sun illuminated bathymetry from the 2003 survey. This map is from section PS1.

The graph below shows the depth profile from A-B, the blue line is the depth during the 2005 survey and the pink line is the depth data from the 2003 survey.

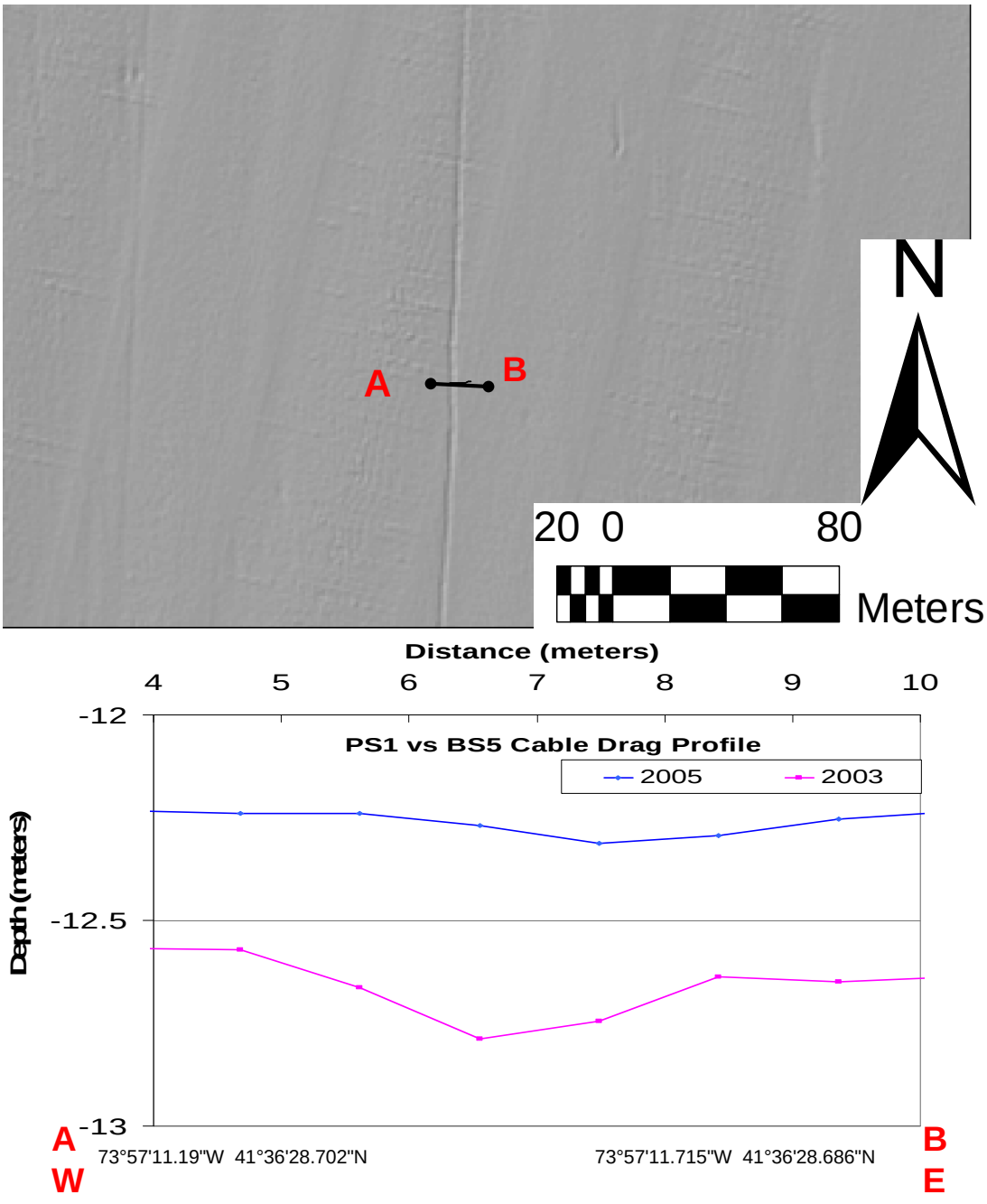
A
B
N
20 0 80
Meters
Distance (meters)
4 5 6 7 8 9 10
-12
-12.5
-13
Depth (meters)
PS1 vs BS5 Cable Drag Profile
2005
2003
A
W
73°57'11.19"W 41°36'28.702"N
73°57'11.715"W 41°36'28.686"N
B
E

Figure 25: The map on the left shows the sun illuminated bathymetry from the 2003 survey. The map on the right shows the sun illuminated bathymetry from the 2005 survey (dark grey) on top of the 2003 sun illuminated bathymetry from 2003 (light grey). These maps are from section PO.

The graph below shows the depth profile from A-B, the blue line is the depth during the 2005 survey and the pink line is the depth data from the 2003 survey.

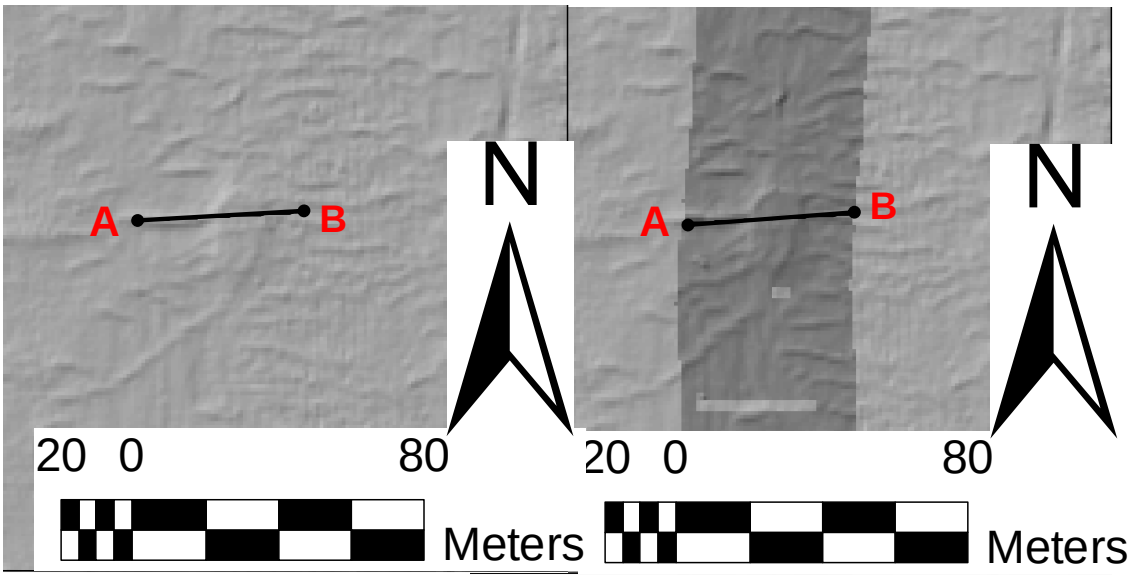
A
B
N
20 0 80
Meters
A
B
N
20 0 80
Meters

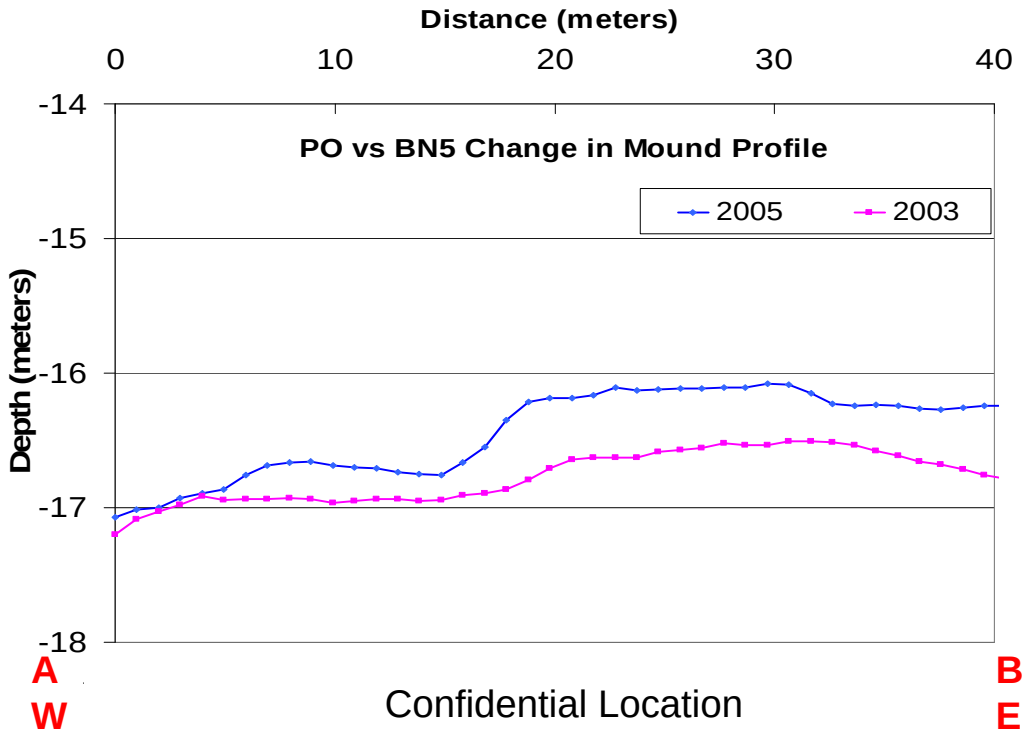
Distance (meters)
0
10
20
30
40
PO vs BN5 Change in Mound Profile
2005
2003
Depth (meters)
-14
-15
-16
-17
-18
A
W
Confidential Location
B
E

Figure 26: Van Rijn equation plots of critical velocity versus water depth (m) for 0.25 mm, 0.5 mm, and 1.0 mm sediment corresponding to fine-very fine, fine-medium, and medium-course sized sand. Reported in phi (Φ) sizes, these sediments correspond to 2 Φ, 1Φ and 0.0 Φ respectively.

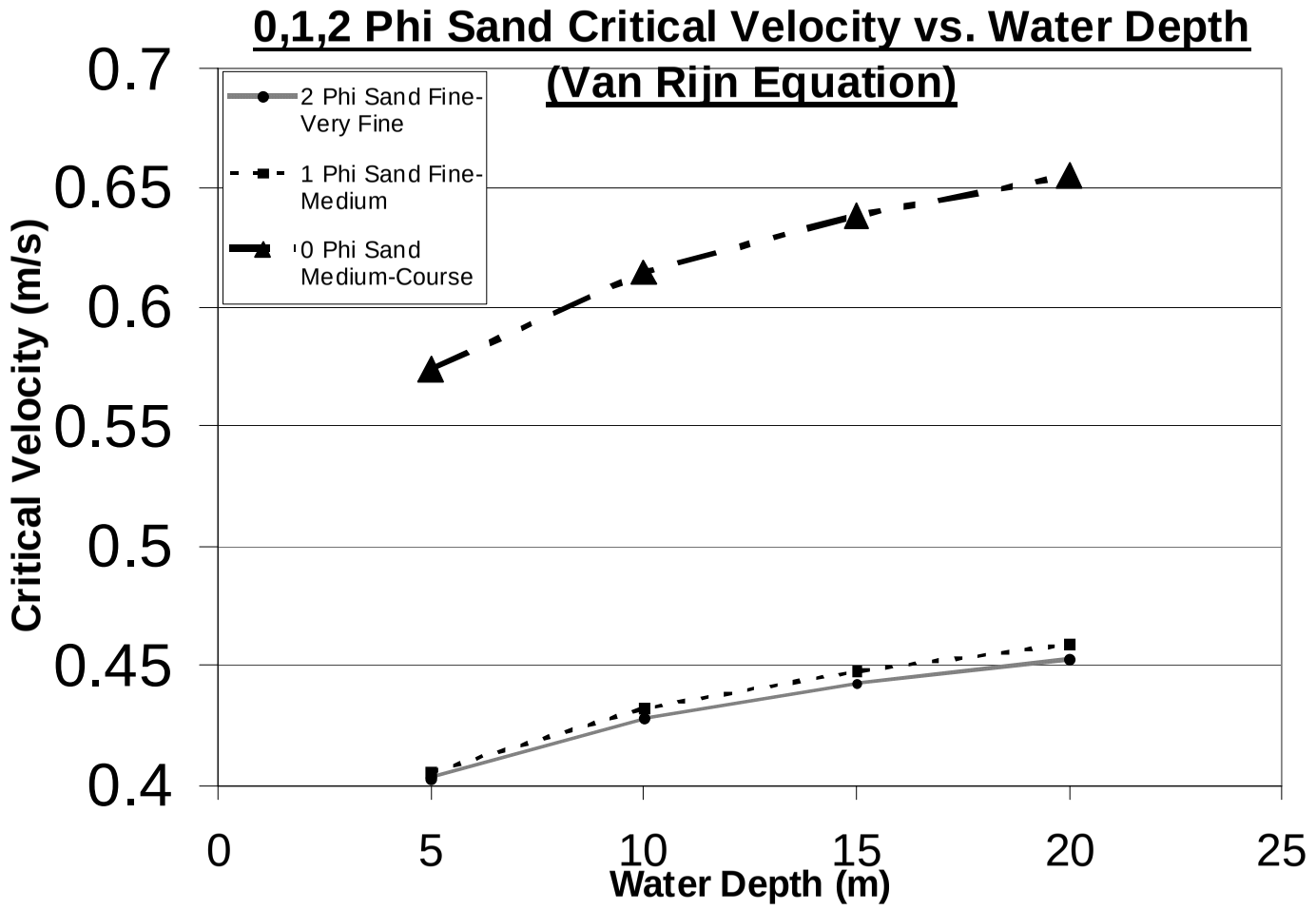
0,1,2 Phi Sand Critical Velocity vs. Water Depth
(Van Rijn Equation)
2 Phi Sand Fine-Very Fine
1 Phi Sand Fine-Medium
0 Phi Sand Medium-Course
Critical Velocity (m/s)
0.7
0.65
0.6
0.55
0.5
0.45
0.4
0
5
10
15
20
25
Water Depth (m)